

This is an Open Access document downloaded from ORCA, Cardiff University's institutional repository: <https://orca.cardiff.ac.uk/id/eprint/143948/>

This is the author's version of a work that was submitted to / accepted for publication.

Citation for final published version:

Gleeson, Matthew, Soderman, Caroline, Matthews, Simon, Cottaar, Sanne and Gibson, Sally 2021. Geochemical constraints on the structure of the Earth's deep mantle and the origin of the LLSVPs. *Geochemistry, Geophysics, Geosystems* 22 (9), e2021GC009932. 10.1029/2021GC009932

Publishers page: <https://doi.org/10.1029/2021GC009932>

Please note:

Changes made as a result of publishing processes such as copy-editing, formatting and page numbers may not be reflected in this version. For the definitive version of this publication, please refer to the published source. You are advised to consult the publisher's version if you wish to cite this paper.

This version is being made available in accordance with publisher policies. See <http://orca.cf.ac.uk/policies.html> for usage policies. Copyright and moral rights for publications made available in ORCA are retained by the copyright holders.



Geochemical constraints on the structure of the Earth's deep mantle and the origin of the LLSVPs

Matthew Gleeson¹, Caroline Soderman², Simon Matthews³, Sanne Cottaar², Sally Gibson²

¹School of Earth and Environmental Sciences, Cardiff University, Main Building, Park Place, CF10 3AT, UK.

²Department of Earth Sciences, University of Cambridge, Downing Street, Cambridge, CB2 3EQ, UK.

³Institute of Earth Sciences, University of Iceland, Sturlugata 7, 102 Reykjavik, Iceland.

KEY POINTS

1. Compositional variability in erupted basalts and olivine crystals reveals the distribution of recycled material in the Galápagos plume.
2. The eastern Pacific LLSVP does not represent piles of subducted oceanic crust.
3. Geochemical and geophysical data indicate the presence of recycled crustal material near the eastern margin of the Pacific LLSVP.

ABSTRACT

Geophysical analysis of the Earth's lower mantle has revealed the presence of two superstructures characterized by low shear wave velocities on the core-mantle boundary. These Large Low Shear velocity Provinces (LLSVPs) play a crucial role in the dynamics of the lower mantle and act as the source region for deep-seated mantle plumes. However, their origin, and the characteristics of the surrounding deep mantle, remain enigmatic. Mantle plumes located above the margins of the LLSVPs display evidence for the presence of this deep-seated, thermally and/or chemically heterogeneous mantle material ascending into the melting region. As a result, analysis of the spatial geochemical heterogeneity in OIBs provides constraints on the structure of the Earth's lower mantle and the origin of the LLSVPs. In this study, we focus on the Galápagos Archipelago in the eastern Pacific, where bilateral asymmetry in the radiogenic isotopic composition of erupted basalts has

This article has been accepted for publication and undergone full peer review but has not been through the copyediting, typesetting, pagination and proofreading process, which may lead to differences between this version and the [Version of Record](#). Please cite this article as [doi: 10.1029/2021GC009932](https://doi.org/10.1029/2021GC009932).

This article is protected by copyright. All rights reserved.

Accepted Article

been linked to the presence of LLSVP material in the underlying plume. We show, using spatial variations in the major element contents of high-MgO basalts, that the isotopically enriched southwestern region of the Galápagos mantle – assigned to melting of LLSVP material – displays no evidence for lithological heterogeneity in the mantle source. As such, it is unlikely that the Pacific LLSVP represents a pile of subducted oceanic crust. Clear evidence for a lithologically heterogeneous mantle source is, however, found in the north-central Galápagos, indicating that a recycled crustal component is present near the eastern margin of the Pacific LLSVP, consistent with seismic observations.

PLAIN LANGUAGE SUMMARY

The Earth's lowermost mantle is characterized by the presence of two superstructures known as the Large Low Shear Velocity Provinces, or LLSVPs. These bodies are characterized by anomalously slow seismic shear wave velocities, may be denser than their surroundings and play an important role in mantle dynamics. However, the origin of these deep mantle structures remains unclear. In this study, we use geochemical data from the Galápagos Archipelago, which is formed through melting of an upwelling mantle plume that contains LLSVP material, to demonstrate that the Pacific LLSVP is not composed of subducted oceanic crust that has accumulated on the core-mantle boundary (as has previously been hypothesized).

1 INTRODUCTION

Volcanic archipelagos such as the Galápagos, Hawai'i and Samoa represent the surface expression of deep-seated mantle plumes that likely originate near the core-mantle boundary (Morgan, 1971; Wilson, 1973). Such regions of ocean island volcanism provide an important window into the composition and structure of the Earth's lower mantle, which plays a critical role in the geodynamical and thermochemical evolution of the planet. For example, unradiogenic He (and Ne) isotope systematics (that is, $^3\text{He}/^4\text{He} > 8 R/R_A$; where R/R_A indicates the measured ratio of $^3\text{He}/^4\text{He}$

relative to the $^3\text{He}/^4\text{He}$ ratio of air) in ocean island basalts (OIBs) indicates that an undegassed, primordial component is likely preserved in the lower mantle over >4 billion years despite vigorous mantle convection (Farley et al., 1992; Jackson et al., 2010; Kurz and Geist, 1999; Stuart et al., 2003). In addition, the radiogenic isotope variability of OIBs provides evidence for recycling of lithospheric material into the deep mantle, resulting in the presence of several isotopically distinct mantle reservoirs (e.g. EM-1, EM-2, HIMU; Chauvel et al., 1992; Hofmann, 1997; Stracke et al., 2005; White and Hofmann, 1982; Willbold and Stracke, 2006). However, to fully understand the long-term evolution of the Earth's lower mantle, it is necessary to relate the chemical heterogeneities observed in OIBs to the detailed picture of the Earth's lower mantle that has been developed through various geophysical techniques.

Seismic tomography images of the Earth's lower mantle reveal that it is far from homogeneous. Most notably, seismic models highlight the presence of two 'superstructures' on the core mantle boundary that are characterized by lower shear wave velocities than the surrounding mantle (Cottaar and Lekic, 2016; Dziewonski and Woodhouse, 1987; Garnero et al., 2016; Ritsema et al., 2011) and are argued to have higher densities than surroundings (Lau et al., 2017; Moulik and Ekström, 2016) at least at their base (Davaille and Romanowicz, 2020; Richards et al., 2021). These superstructures, known as Large Low Shear Velocity Provinces (LLSVPs), are located beneath Africa and the Pacific and play a critical role in mantle dynamics, the rise of mantle plumes (Heyn et al., 2020), and the configuration of True Polar Wander events (Steinberger et al., 2017). Despite their importance, however, the origin of the LLSVPs remain enigmatic, with their presence having previously been assigned to piles of subducted oceanic crust (Brandenburg and van Keken, 2007; Niu, 2018) or primordial material that has undergone differentiation early in Earth's history (such as magma ocean cumulates; Deschamps et al., 2012; Labrosse et al., 2007; Peters et al., 2018).

Global seismic tomography models reveal that many mantle plumes are rooted within, or at the margins of the LLSVPs, indicating that these regions represent 'plume nurseries' (Fig. 1; Doubrovine

et al., 2016; French and Romanowicz, 2015; Jackson et al., 2018). Furthermore, several mantle plumes worldwide display bilateral asymmetry; where isotopically enriched signals are assigned to melting of upwelling LLSVP material, and isotopically depleted compositions are related to melting of the surrounding peridotitic mantle (Harpp et al., 2014b; Harpp and Weis, 2020; Hoernle et al., 2015; Huang et al., 2011; Weis et al., 2011; Zhou et al., 2020). Therefore, a critical analysis of the compositional variability displayed by one such mantle plume, considering all available isotopic, trace element and major element data, has the potential to reveal new insights into the origin of the LLSVPs, with implications for the evolution of the solid Earth over billion-year timescales. Specifically, correlation of the isotopic and lithological heterogeneity (the latter inferred by major elements in basalts and minor elements in olivine) observed in LLSVP-rooted plumes will allow the distribution of recycled components in the lower mantle to be investigated and thus determine whether LLSVPs truly represent piles of subducted oceanic crust.

Here, we choose to focus on the Galápagos Archipelago, which is located above the eastern margin of the Pacific LLSVP and displays bilateral asymmetry in the trace element and radiogenic isotope composition of the erupted basalts (Harpp et al., 2014b; Harpp and Weis, 2020). We present new olivine data from the central Galápagos that, alongside published olivine and whole-rock data from across the archipelago, allows us to determine the spatial variability in the lithological structure of the underlying mantle plume. In doing so, we identify where recycled crustal components are directly involved in the genesis of Galápagos magmas (Herzberg, 2011; Rosenthal et al., 2015; Sobolev et al., 2005; Yaxley and Green, 1998). Finally, we discuss the implications of our findings for the structure of the lower mantle beneath the Pacific and the origin of the Pacific LLSVP.

2 GEOLOGICAL BACKGROUND

The Galápagos Archipelago is located ~1000 km off the western coast of Ecuador in the eastern equatorial Pacific and represents one of the most volcanically active regions in the world. Volcanism in the Galápagos is driven by melting in an upwelling mantle plume that has a mantle potential

temperature (T_P) >30 – 150 °C above that of the ambient mantle (Gibson et al., 2015). Seismic tomography provides evidence that the Galápagos mantle plume originates below the mantle transition zone, likely at the core-mantle boundary near the eastern margin of the Pacific LLSVP (Hoofst et al., 2003; Nolet et al., 2019).

The Galápagos Archipelago lies on the eastward-moving Nazca tectonic plate (plate velocity of ~50 km/Myr; Argus et al., 2011), about 150 – 200 km south of the Galápagos Spreading Centre, a plume-influenced segment of the global mid-ocean ridge system. Seismic tomography indicates that the Galápagos mantle plume is centered beneath the south-western Archipelago at ~200 km depth, but is deflected to the north-east at ~100 – 80 km depth owing to the presence of the nearby spreading centre (Villagómez et al., 2014). The Galápagos Spreading Centre itself clearly shows the influence of the nearby mantle plume in the geochemical composition of the erupted basalts and the crustal thickness of the ridge (Canales et al., 2002; Christie et al., 2005; Cushman et al., 2004; Detrick et al., 2002; Gibson and Richards, 2018; Gleeson et al., 2020; Gleeson and Gibson (2021); Ingle et al., 2010; Schilling et al., 1982; Sinton et al., 2003).

Owing to the west-to-east motion of the Nazca tectonic plate, Galápagos volcanoes follow a general west-to-east age progression, with the youngest volcanic activity in the west and the oldest lavas observed on the eastern islands of San Cristobal and Espanola (Bailey, 1976; Geist et al., 1986; Naumann and Geist, 2000). However, volcanic activity in the central and eastern Galápagos persists into the Holocene, with historical eruptions observed on the central island of Santiago (Global Volcanism Program, 2013) and lavas as young as ~9 ka found on the eastern-most island of San Cristobal (Mahr et al., 2016). Nevertheless, some of the basalts from the eastern-most Galápagos may have erupted when the islands were located several 10s of km west of their current location. Yet, owing to the size of the Galápagos Archipelago (>400 km from west to east), and the dominance of more recent volcanic activity on the central and western Galápagos volcanoes, the composition of

basalts erupted across the Galápagos Archipelago can be used to evaluate the spatial heterogeneity of the underlying mantle plume.

2.1 ISOTOPIC HETEROGENEITY OF THE GALÁPAGOS ARCHIPELAGO

Since the 1980s, analysis of radiogenic isotope ratios has dominated understanding of source

heterogeneity in the Galápagos mantle plume (Geist et al., 1988; Harpp and Weis, 2020; Harpp and White, 2001; Hoernle et al., 2000; White et al., 1993). Specifically, spatial variability in the Pb, Nd, Hf and Sr isotope composition of the Galápagos basalts has traditionally been interpreted to represent the contribution of melts from at least 4 isotopically distinct end-members (Blichert-Toft and White, 2001; Harpp and White, 2001). These end-members, known as PLUME, FLO, WD (Wolf-Darwin), and DGM (Depleted Galápagos Mantle), are most strongly expressed in spatially defined regions of the Galápagos Archipelago and associated ridges (Harpp and White, 2001; Hoernle et al., 2000).

The PLUME end-member is dominant in basalts from the westernmost island of Fernandina, and is characterized by moderately radiogenic Sr and Pb isotope signatures, similar to the common plume component referred to as 'FOZO' or 'C' (Hanan and Graham, 1996; Harpp and White, 2001). Notably, the Fernandina basalts have unradiogenic He and Ne isotope signatures (e.g. $^3\text{He}/^4\text{He}$ up to 30 R/R_A; Kurz and Geist, 1999), which indicates the presence of an undegassed primordial reservoir in the Galápagos plume.

To the south of Fernandina, basalts trend towards more radiogenic Sr and Pb isotope signatures, which reach a maximum on the southern island of Floreana (Harpp et al., 2014a; Harpp and White, 2001; Kurz and Geist, 1999). The extreme radiogenic isotope composition of Floreana (that is, elevated $^{206}\text{Pb}/^{204}\text{Pb}$ and $^{187}\text{Os}/^{188}\text{Os}$ ratios) is used to define the FLO mantle end-member, which displays similar $^{206}\text{Pb}/^{204}\text{Pb}$ signatures to the global HIMU mantle (Gibson et al., 2016; Harpp et al., 2014a). As a result, the FLO mantle is hypothesized to represent recycled Archean oceanic crust (Gibson et al., 2016; Harpp et al., 2014a), although the absence of evidence for a pyroxene-rich

component in the mantle source of the Floreana lavas casts doubt on the recycled crustal origin (Gleeson et al., 2021; Vidito et al., 2013).

Basalts in the eastern Galápagos (i.e. Genovesa, San Cristobal and eastern Santiago) are dominated by melts of the DGM (Gibson et al., 2012; Harpp and White, 2001). However, whether the DGM component is entrained upper mantle, or derives from the lower mantle, is an ongoing area of debate (Blichert-Toft and White, 2001; Gibson et al., 2012; Harpp and Weis, 2020; Hoernle et al., 2000). Finally, the WD isotopic end-member is restricted to a small number of seamounts and minor islands in the northernmost Galápagos and appears to have little to no influence on the composition of basalts elsewhere in the Galápagos (Harpp and White, 2001). The origin of this localized component is unknown and is not addressed in this study.

The complex relationship between the different mantle end-members identified in the Galápagos mantle plume has made correlation of these signatures to the structure of the underlying deep mantle very challenging. It is possible, however, to simplify the spatial heterogeneity observed in the radiogenic isotope composition of the Galápagos basalts and instead describe their variability in terms of overall isotopic enrichment (Harpp and Weis, 2020). The most enriched isotopic signatures (here used to describe radiogenic Pb and Sr and unradiogenic Nd isotope compositions) are observed in the western and southern Galápagos, whereas isotopically depleted compositions dominate in the north-eastern Galápagos (apart from Pinta, whose anomalously enriched composition is likely related to plume-ridge interactions in the Galápagos; Fig. 2a).

Critically, this isotopic variability mirrors the structure of the deep mantle at the base of the Galápagos mantle plume, with LLSVP material to the south-west and 'normal' lower mantle to the north-east (Fig. 1 & 2; Cottaar and Lekic, 2016; Garnero et al., 2016; Ritsema et al., 2011). As a result, the enriched isotopic signatures of the south-western Galápagos have been assigned to melting of LLSVP material ascending as part of the Galápagos mantle plume, whereas the depleted nature of

the north-eastern Galápagos basalts is hypothesized to result from melting of the surrounding peridotitic mantle (Harpp et al., 2014b; Harpp and Weis, 2020).

2.2 LITHOLOGICAL PROPERTIES OF THE GALÁPAGOS MANTLE PLUME

Our current understanding of the structure and composition of the Galápagos mantle plume is complicated by the unclear relationship between lithological and radiogenic isotopic heterogeneity (Gleeson et al., 2020; Gleeson and Gibson, 2019; Vidito et al., 2013). Lithological heterogeneity, that is, the presence of fusible, pyroxene-rich components in the underlying mantle, is believed to result from recycled crustal components in the mantle and their incorporation into upwelling mantle plumes (Gibson, 2002; Hauri, 1996; Lambart, 2017; Lambart et al., 2013; Mallik and Dasgupta, 2012; Rosenthal et al., 2015; Shorttle et al., 2014; Sobolev et al., 2007, 2005; Yaxley and Green, 1998). As such, identification of lithological heterogeneity in the mantle source region of basaltic lavas provides evidence for the contribution of recycled crustal components to mantle plumes. Therefore, linking signatures of lithological heterogeneity to the isotopic heterogeneity of the Galápagos mantle plume might help to identify whether the LLSVPs truly represent piles of subducted oceanic crust.

Lithological heterogeneity in the mantle is commonly tracked through the minor element composition of olivine phenocrysts (Gurenko et al., 2013, 2009; Herzberg, 2011; Sobolev et al., 2007, 2005). Specifically, high Ni but low Mn and Ca contents in primitive olivine phenocrysts are thought to be characteristic of a contribution from pyroxenite-derived melts, owing to the large differences in the bulk partition coefficient of these elements during melting of an olivine-rich (peridotite) and a pyroxene-rich (pyroxenite) lithology.

The composition of olivine crystals from the Galápagos Archipelago has previously been used to evaluate the lithological structure of the underlying plume, with initial interpretations suggesting that lithologically distinct components are present in both isotopically enriched and isotopically depleted regions of the Galápagos (Vidito et al., 2013). However, the presence of a pyroxenitic component in the mantle source region of the eastern Galápagos basalts contradicts their

isotopically depleted nature and trace element systematics (e.g. Gibson et al., 2012). As a result, the anomalously high Ni and low Ca contents of the eastern Galápagos olivines were recently revisited, with numerical models of fractional crystallisation, magma recharge and diffusive re-equilibration demonstrating that these 'pyroxenitic' olivine compositions could be generated through crustal processing of basaltic lavas (Gleeson and Gibson, 2019).

Nevertheless, it remains possible that pyroxenitic source components contribute to basalts from other regions of the Galápagos. In fact, analysis of Fe-isotope ratios in basaltic lavas from plume-influenced regions of the Galápagos Spreading Centre (GSC) revealed that an enriched pyroxenitic component is present in the Galápagos mantle plume (Gleeson et al., 2020). However, it remains uncertain whether the enriched pyroxenite in the mantle source region of the GSC basalts is related to the isotopically enriched signatures assigned to melting of the LLSVP material contained within the Galápagos mantle plume. To address this, we collect new olivine data from the central Galápagos, which is used alongside published olivine and whole-rock data from across the Galápagos Archipelago to evaluate the spatial variability in the lithological properties of the underlying mantle.

3 METHODS

We present high-precision analyses of the major and minor element composition of olivine crystals in geochemically enriched basalts from western Santiago in the central Galápagos. Previous work on the major element, trace element and isotopic composition of the Santiago basalts has led to the classification of four chemical groups: low-K tholeiites, high ϵNd transitional basalts, low ϵNd transitional basalts, and mildly-alkaline basalts (Gibson et al., 2012). In general, the low-K tholeiites are found on the eastern side of the island, with enriched isotopic signatures found in mildly-alkaline basalts further west (Gibson et al., 2012). Our new data from well-characterised mildly alkaline and low ϵNd transitional basalts fills a crucial gap in the olivine data from the Galápagos, as olivine compositions from western and eastern Galápagos basalts (including eastern Santiago) have previously been characterized (Gleeson and Gibson, 2019; Vidito et al., 2013).

All data were collected using a Cameca SX100 electron microprobe in the Department of Earth Sciences, University of Cambridge. Analysis was carried out using a defocused (5 μm) spot and a 15 kV accelerating voltage. Analysis of Si, Fe, and Mg was carried out using a 20 nA beam current. To increase the analytical precision on low concentration elements, a 100 nA beam current was used for analysis of Ni, Mn, Ca and Al. Mineral and metal standards were used to calibrate at the start of the analytical session and precision and accuracy were tracked through repeat analysis of a San Carlos Olivine secondary standard. Recovery for all elements is between 99 and 103%. The 2-sigma analytical precision of analysis is $\sim 3\%$ for Fe, better than 1.5% for Mg and Si, $\sim 4\%$ for Ni, $\sim 15\%$ for Ca, and $\sim 8\%$ for Mn (Supplementary Data).

4 RESULTS

Our new analyses reveal that olivines in mildly alkaline basalts from Isla Santiago (such as sample 08DSG33) are relatively evolved, with forsterite (Fo) contents ranging from $\sim 70 - 84$, and contain moderately high Ni contents ($\sim 800 - 2900$ ppm; Fig. 3). Olivines in mildly alkaline basalts also contain relatively low Mn contents ($\sim 1500 - 2500$ ppm), and correspondingly high Fe/Mn ratios (72.8 ± 5.2 ; Fig. 3). In contrast, the Fo contents of olivines from transitional basalt 07DSG61 are slightly more primitive than those observed in the mildly alkaline basalts (Fo $\sim 81-85$). Furthermore, the Ni content and Fe/Mn ratio of olivines in sample 07DSG61 are lower than those observed in the mildly alkaline basalts ($\sim 1200 - 2300$ ppm and 71.1 ± 5.1 , respectively; Fig. 3).

5 DISCUSSION

5.1 OLIVINE MINOR ELEMENT SYSTEMATICS

Olivine minor elements provide a powerful method for investigating the lithological properties of the mantle (Gurenko et al., 2009; Herzberg et al., 2014; Sobolev et al., 2007), as long as the influence of crustal processes and the conditions of mantle melting are considered (Gleeson and Gibson, 2019; Matzen et al., 2013, 2017b). Olivine data from the eastern Galápagos (that is, San Cristobal,

Genovesa and Espanola) indicate that the mantle source regions of these basalts are dominated by peridotite (Vidito et al., 2013; Fig. 3a,b). However, interpretation of olivine data from elsewhere in the Galápagos is not so simple (Gleeson and Gibson, 2019).

Taken at face value, the Ca content (and to a lesser extent the Ni content) of olivines in basalts from Floreana in the southern Galápagos, which originates from melting of LLSVP material with highly radiogenic Pb isotope signatures (Harpp and Weis, 2020), suggests that there is a notable contribution from melts from a pyroxenitic source component (Gleeson et al., 2021; Harpp et al., 2014a; Vidito et al., 2013). However, the low Ca contents and moderately high Ni contents observed in some of the Floreana olivines can instead be explained by chemical modification in a cumulate mush (Gleeson et al., 2021). As such, there is no significant evidence in the olivine minor element systematics of the Floreana basalts to indicate that there is a substantial contribution of melts from a pyroxenitic source component (Fig. 3).

Olivine data from the western Galápagos (that is, the islands of Isabela, Roca Redonda, and Fernandina) display a range of compositions. Notably, it is clear that the Ni, Fe/Mn and Ca contents of olivines from Fernandina and Cerro Azul (on the southern margin of Isabela), which fall into the isotopically enriched south-western region of the archipelago, are consistent with the presence of a peridotite source (especially once the influence of crustal processes are taken into account; Gleeson and Gibson, 2019; Vidito et al., 2013). However, evidence for the contribution of melts from a pyroxenitic source component is found in the Fe/Mn ratio of olivines from Roca Redonda and Volcans Ecuador, Wolf and Darwin on Northern Isabela (Fe/Mn >70; Fig. 3 & 4; Vidito et al., 2013). Notably, the Ni contents of olivine from Roca Redonda and Volcan Ecuador are also higher than the olivine compositions predicted by the magma mixing models of Gleeson and Gibson (2019), supporting the interpretation that a pyroxenitic source contributes to the olivine composition of these Northern Isabela and Roca Redonda basalts. High Fe/Mn ratios (>75) are also found in olivines from Sierra Negra, but the evolved nature of the Sierra Negra basalts (often <5 wt% MgO) and

olivines mean that we cannot rule out these signatures originating through crustal processing (cf. Trela et al., 2015).

In the central Galápagos, olivine data from mildly-alkaline basalts E-76 and 08GSD33 on western Santiago, reveal Ni and Fe/Mn contents that are too high to be explained by melting of a peridotitic source, even if the influence of crustal processes are considered (Gleeson and Gibson, 2019).

Although care must be used when comparing the composition of magmatic olivines to the composition of their host basalt, as olivine crystals might not be directly related to their carrier melt (Wieser et al., 2019), it is notable that these basalts display the most enriched trace element and isotopic signatures of any basalt found on Santiago (Gibson et al., 2012). Conversely, olivine data from isotopically depleted basalts on eastern Santiago are consistent with a dominant contribution of melts from a peridotitic source lithology (Gibson et al., 2016; Gleeson and Gibson, 2019).

Transitional basalts from Santiago (such as 07DSG61) display intermediate olivine compositions at moderately high Ni and Fe/Mn contents, confirming that these basalts represent a mixture of pyroxenite and peridotite derived melts.

Olivine compositions from Santa Cruz in the central Galápagos fall into two groups, although the compositions measured within each sample are typically relatively uniform (Vidito et al., 2013). One group displays Fe/Mn contents between 60 and 72 (that is, consistent with a peridotitic source; Herzberg, 2011), whereas the other contains Fe/Mn ratios >70 . The high Fe/Mn group also contains high Ni contents that cannot be easily explained by crustal processing of peridotite-derived basaltic magmas (Gleeson and Gibson, 2019). As such, the variability in the olivine composition of basalts from Santa Cruz likely results from changes in the proportion of pyroxenite-derived melt. The olivine compositional characteristics of Santa Cruz does not appear to define a geographic geochemical trend, unlike on Santiago (Gibson et al., 2012), with shorter length-scale variability in the composition of erupted basalts dominating.

Overall, the new and compiled olivine data indicates that a pyroxenitic, recycled component is present in the Galápagos mantle plume. However, this pyroxenitic component is not dominant in basalts of the isotopically enriched south-western region of the Galápagos. Instead, it is most prevalent in basalts from the north-central Galápagos, that is, mildly-enriched basalts from northern Isabela, Roca Redonda, western Santiago, and Santa Cruz (Fig. 4a). Importantly, our results indicate that geochemically enriched peridotite and pyroxenite components exist in the Galápagos mantle plume; as a result, there is no simple relationship between host-basalt enrichment and olivine Ni and Mn contents across the archipelago. Nevertheless, the proposed contribution of pyroxenitic melts to the north-central Galápagos basalts is supported by the isotopic similarity of these basalts (with regards to Sr, Nd and Pb) to the pyroxenitic end-member previously identified in the mantle source region of the GSC basalts (Gleeson et al., 2020; Gleeson and Gibson, 2021; Fig. 5).

5.2 MAJOR ELEMENT SYSTEMATICS OF THE GALÁPAGOS BASALTS

Alongside olivine minor element compositions and Fe-isotope ratios of basaltic lavas, information about the lithological properties of the mantle source is contained in the major element systematics of high-MgO basalts (i.e., those that have not undergone significant fractionation of clinopyroxene or plagioclase; Dasgupta et al., 2010; Hauri, 1996; Lambart et al., 2016, 2013; Shorttle et al., 2014; Shorttle and Maclennan, 2011). Specifically, melts of a pyroxenitic source lithology often have lower CaO contents, and higher FeO_t contents (where FeO_t represents the total Fe content of the melt expressed as FeO), than melts of a peridotite (Herzberg, 2011; Hirose and Kushiro, 1993; Lambart et al., 2016, 2012).

To evaluate the spatial variability in the major element composition of primary mantle melts from the Galápagos, we compiled whole-rock major element data from across the archipelago and filtered the resulting dataset to exclude any samples with MgO contents <8 wt% (i.e., those that display substantial evidence for clinopyroxene and plagioclase fractionation; see Supplementary Information). Basalts in the filtered database contain a relatively narrow range of Mg# compositions

(from ~55 to ~75 where $Mg\# = Mg/(Mg+Fe_t)$ molar). However, variations in other major element parameters are observed.

Notably, the FeO_t content of high-MgO basalts from the western, southern and eastern Galápagos are consistently <11 wt%, and typically less than 10.5 wt%. Melting experiments at pressures between 1.5 and 3 GPa on the KLB-1 peridotite (a commonly used experimental analogue for the upper mantle) provide mean FeO_t contents of 8.88 wt%, and maximum FeO_t contents of 10.05 wt%, broadly consistent with the compositions observed in the western, southern and eastern Galápagos (Fig. 2b; Fig. 4; Hirose and Kushiro, 1993; Takahashi et al., 1993). Furthermore, melting calculations performed in the KNCFMASr system using THERMOCALC v3.4.7 reveal that melts produced by the KLB-1 peridotite between 1.5 and 3 GPa, and at melt fractions less than 20% (see Supplementary Information), contain approximately $9.77^{+1.09}_{-1.99}$ wt% FeO_t (Holland et al., 2018; Holland and Powell, 2011; Powell et al., 1998), almost perfectly overlapping with the FeO_t content of the western, southern and eastern Galápagos basalts ($9.74^{+0.94}_{-0.98}$ wt% FeO_t ; Fig. 4). Melts produced in hydrous melting regimes at significantly higher pressures (>3 GPa) are volumetrically minor, and therefore unlikely to influence the major element systematics of the Galápagos basalts and not considered here. In addition, the CaO contents of primitive basaltic magmas in the southern, eastern and western Galápagos are also consistent with the CaO content predicted from melting of a peridotite source (Hirose and Kushiro, 1993; Takahashi et al., 1993). As such, basalts in these regions of the Galápagos are likely dominated by melts of a peridotite source, with only a minor-to-moderate contribution from melts of a pyroxenitic component (<0 - 30 %), broadly consistent with the compositions observed in olivine crystals from these basalts (see above).

Some basalts in the north-central Galápagos, that is, Santa Cruz and western Santiago, the northern margin of Isabela (Volcan Ecuador) and Roca Redonda, display FeO_t contents >11 wt%. In fact, on western Santiago and Roca Redonda, the whole-rock FeO_t contents extend to >12.5 wt%, well outside the range of FeO_t contents that can result from melting of a peridotite source lithology (Fig.

4; Gibson et al., 2000; Hirose and Kushiro, 1993). Even if basalts from Roca Redonda with MgO contents >15 wt%, which may have assimilated high-FeO_t olivine, are excluded the whole-rock FeO_t contents of the remaining basalts are notably higher than those of the south-western and eastern Galápagos (~11 – 12 wt%; Supplementary Information). In addition, it is unlikely that a substantial increase in the depth of melting beneath the north-central Galápagos (relative to the western Galápagos) could explain this shift to higher FeO_t contents, as the lithosphere is thickest and the mantle potential temperature is greatest beneath the south-western region of the archipelago where low FeO_t values are observed (Gibson and Geist, 2010).

The high FeO_t contents of the north-central Galápagos are consistent with the FeO_t concentrations measured in experimental melts of pyroxenitic lithologies such as MIX-1g and M5-40 (Hirschmann et al., 2003; Kogiso et al., 2003; Lambart et al., 2013). Melting simulations in THERMOCALC v3.4.7 again support the experimental data, and demonstrate that melts of MIX-1g at pressures above 1.5 GPa, and melt fractions below 60%, contain $11.54^{+2.22}_{-1.88}$ wt% FeO_t, indicating a strong contribution of melts from a pyroxenitic source to the basalts of the north-central Galápagos ($10.95^{+1.44}_{-1.13}$ wt% FeO_t; Fig. 4). Notably, the regions of the northern and central Galápagos that display basalt FeO_t contents >11 wt% all plot very close to the region where olivine minor element chemistry indicates the presence of a recycled pyroxenitic source component (Fig. 3 & 4).

In addition, a more detailed look at the central Galápagos (that is, Santiago, Santa Cruz, Santa Fe and Rabida), demonstrates that the major element variability observed across the Galápagos Archipelago is related to the degree of trace element and isotopic enrichment (Fig. 6 & 7). For example, high-MgO basalts with high FeO_t and low CaO contents, which are inconsistent with the composition of melts produced by a peridotite source, are typically characterized by moderately radiogenic Pb and Sr isotope ratios and enriched trace element systematics (e.g. Nb/Y > 0.4; Gibson et al., 2012). Furthermore, comparison of experimental melt compositions to the observed major element systematics of the central Galápagos basalts has previously shown that the compositional variations

across Isla Santiago are consistent with the presence of both pyroxenite and peridotite components in the mantle source, an observation that is consistent with the THERMOCALC v3.4.7 calculations presented here (Supplementary Information; Gleeson et al., 2020).

The high FeO_t contents of the central Galápagos and Northern Isabela/Roca Redonda basalts are also expressed in their anomalously high Fe/Mn ratios (>65 ; Fig. 5b). However, unlike the FeO_t and CaO contents of basalts from across the Galápagos Archipelago, there is a slight difference in the Fe/Mn ratio of basalts from the western Galápagos (Fernandina and Southern Isabela; ~ 60) and the eastern Galápagos (Espanola and San Cristobal; ~ 55). Variations in the Fe/Mn ratio of basaltic magmas have traditionally been assigned to the presence of a fusible, pyroxenitic component (Herzberg, 2011) or a core component (Humayun et al., 2004) in the mantle source. Yet, the slight variation in the Fe/Mn ratio of the western and eastern Galápagos basalts could be explained by differences in the depth of melting (Matzen et al., 2017a), consistent with the greater lithospheric thickness in the western Galápagos compared to the eastern Galápagos (Gibson et al., 2012; Gibson and Geist, 2010). Nevertheless, the higher Fe/Mn ratio of the north-central Galápagos basalts requires a substantial contribution from melts of a pyroxenitic source, as these signatures cannot be generated by variations in the melting processes alone (Fig. 5b).

Overall, variations in the major element systematics of primitive basaltic lavas from across the Galápagos Archipelago indicate that a pyroxenitic component is present in the underlying mantle plume and is most strongly expressed in the composition of basalts from the north-central Galápagos basalts (northern Isabela, Roca Redonda, western Santiago and Santa Cruz). This hypothesis is supported by the similarity between the radiogenic isotope composition of the most enriched basalts from the north-central Galápagos (on Roca Redonda and western Santiago; Standish et al., 1998; Gibson et al. 2012) and the proposed isotopic composition of the pyroxenitic end-member in the mantle source region of the GSC basalts (Fig. 5; Gleeson et al., 2020; Gleeson and Gibson, 2021). As a result, the major element systematics of the primitive Galápagos basalts

indicate that an isotopically enriched pyroxenitic source component contributes to both basalts from the north-central Galápagos, consistent with our interpretations based on the available olivine data shown above, and the GSC.

The spread of isotopic compositions observed in basalts from both the south-western and eastern Galápagos indicates that a small contribution of Sr, Pb and Nd-rich melts from this pyroxenitic component (i.e., <25% pyroxenitic melt) might influence the radiogenic isotope ratios of basalts erupted across the entire archipelago (Fig. 8). There is, however, no evidence in the major element systematics of basalts from Fernandina, Southern Isabela and Floreana to indicate that there is a large contribution of melts from this pyroxenitic component to the major element composition of basalts in the isotopically enriched south-western region of the archipelago (Fig. 4). Additionally, the major element systematics of the eastern Galápagos basalts provide no evidence to support previous interpretations of a depleted pyroxenitic component is dominant in the eastern Galápagos (Vidito et al., 2013).

5.3 VARIATIONS IN SOURCE PYROXENITE PROPORTIONS

The major element systematics of high-MgO basalts, and the minor element contents of their olivine cargo, reveal clear variations in the contribution of pyroxenitic melts to basalts erupted across the Galápagos Archipelago. However, it is important to consider whether the prevalence of pyroxenitic melt signatures in the north-central region of the Galápagos represents true spatial heterogeneity in the distribution of pyroxenitic components in the underlying Galápagos mantle plume, or if these signatures can instead be caused by variations in mantle potential temperature, melt extents, and melt extraction processes. Addressing this question is critical to understanding the distribution of lithologically distinct, recycled components in the Earth's lower mantle.

As pyroxenitic source components are typically more fusible than 'normal' mantle peridotite, the pyroxenite solidus will be crossed at higher pressures than the peridotite solidus during adiabatic decompression melting (Gibson et al., 2000; Kogiso et al., 2003; Lambart et al., 2016, 2013; Sobolev

et al., 2007; Yaxley and Green, 1998). Therefore, melts of a pyroxenitic source dominate at low total melt fractions during melting of a two- or three-component mantle, with peridotite-derived melts becoming more dominant at shallower pressures (Lambart et al., 2016). As a result, the proportion of pyroxenite-derived melt contributing to the composition of basaltic lavas is influenced by variations in the mantle potential temperature and lithospheric thickness, as well as the proportion of pyroxenite in the source.

To address whether variations in melting parameters could explain the spatial variability in the contribution of pyroxenitic melts to the Galápagos Archipelago, we calculate the proportion of pyroxenite-derived melt that results from melting of a two-component mantle under various conditions. Calculations were performed using the pymelt Python module (Matthews et al., 2020), and recent empirical parameterisations for the melting of a lherzolitic peridotite and silica-undersaturated pyroxenite (KLB-1 and KG1, respectively; Matthews et al., 2021). We ran the calculations over a range of mantle potential temperatures ($T_p = 1400 - 1460$ °C) and lithospheric thicknesses (46 – 60 km; $\sim 1.5 - 1.85$ GPa) appropriate to the Galápagos Archipelago (Gibson et al., 2015, 2012; Gibson and Geist, 2010; Herzberg and Asimow, 2008; Vidito et al., 2013), and consider how these conditions may influence the relative contribution of melts from a mixed peridotite-pyroxenite mantle source. For example, the pymelt models indicate that a mantle containing $\sim 10\%$ pyroxenite, melting at a T_p of 1400 °C under 60 km thick lithosphere produces magmas with a pyroxenite melt proportion of $\sim 70\%$. Melting of the same mantle with a T_p of 1460°C and a lithospheric thickness of ~ 46 km gives a pyroxenitic melt proportion of only $\sim 30\%$.

To determine whether variations in the conditions of mantle melting across the Galápagos Archipelago can cause the observed differences in the relative contribution of pyroxenitic melts to the Galápagos basalts, we compare the results of our melting calculations to first-order estimates of the proportion of pyroxenitic melt that contributes to each region of the Galápagos. These estimates are derived from the mean FeO_t content of the Galápagos basalts, an assumed peridotite melt FeO_t

content of 8.8 – 9.77 wt% and a pyroxenite melt FeO_t content of 12.8 wt% (representing the mean FeO_t content of the experimental and thermodynamic KLB-1 melts and the highest FeO_t content observed in any of the Galápagos basalts, respectively). Results indicate that basalts from the western and eastern Galápagos contain, on average, a 0 – 24% contribution of melts from a pyroxenitic source (mean FeO_t of 9.75 wt%), whereas basalts from western Santiago contain 57 – 80% pyroxenitic melts (FeO_t contents between 11.5 and 12 wt%). This variation is similar in magnitude to the maximum difference in the proportion of pyroxenitic melt that can be caused by variations in the melting conditions of a homogeneous mantle source beneath the Galápagos Archipelago (~30 – 70%; Fig. 9).

Regions of the Galápagos Archipelago that are dominated by melts of peridotitic source lithologies, however, do not only occur in regions where the lithosphere is thinnest or where the mantle potential temperature is highest. For example, Isla Fernandina and Volcan Cerro Azul, on southern Isabela, display no evidence for the contribution of pyroxenitic melts, despite the fact that seismic data indicates the lithosphere is thickest in this region of the archipelago (Fig. 2c; Gibson and Geist, 2010; Rychert et al., 2014). As such, it is unlikely that variations in the contribution of pyroxenitic melts to basalts erupted across the Galápagos Archipelago results purely from variations in the melting conditions. Instead, we suggest that the difference in the proportion of pyroxenitic melt contributing to basalts from the south-western, north-central and north-eastern regions of the Galápagos Archipelago must result from variations in the proportion of pyroxenite present in the mantle source. We note that the first-order estimates for the proportion of pyroxenitic melt contributing to each region of the Galápagos presented above can be recreated when the mantle source region of the western, southern and eastern Galápagos contains <5 % pyroxenite, but the mantle source region of the north-central Galápagos basalts contains >20% pyroxenite (Fig. 9).

In addition, the presence of at least three distinct components in the Galápagos mantle plume are required by the radiogenic isotope variability of the Galápagos basalts. Specifically, we note that the

$^{87}\text{Sr}/^{86}\text{Sr}$ isotope signature of the north-central Galápagos basalts (pyroxenite source) are lower than that observed in basalts from the south-western Galápagos (peridotite source; Fig. 5). This indicates that basalts in the south-western archipelago cannot be a mixture of melts derived from an enriched pyroxenite and a depleted peridotite, otherwise they would display a less enriched radiogenic isotope composition than the basalts from the north-central Galápagos (where the pyroxenitic source component is most strongly expressed). As a result, the presence of one or more isotopically enriched south-western peridotite components are required (Fig. 8), alongside a pyroxenite source component that is focused beneath the north-central Galápagos and an isotopically depleted north-eastern peridotite (Fig. 10).

As indicated above, we cannot exclude the possibility that a small fraction of pyroxenitic material (i.e., <5%) exists in the mantle source of all Galápagos basalts and contributes to their isotopic compositions (Fig. 8). However, the analysis presented here clearly shows that this pyroxenitic component is present in much higher proportions in the mantle source region of the north-central Galápagos basalts, separating the isotopically enriched domain of the south-western Galápagos from the isotopically depleted eastern Galápagos.

6 IMPLICATIONS FOR THE STRUCTURE OF THE DEEP MANTLE

Owing to the location of the Galápagos Archipelago above the eastern margin of the Pacific LLSVP, and the asymmetric structure of the Galápagos mantle plume (with regards to isotopic composition), it is hypothesised that the plume stem is rooted at the eastern boundary of the Pacific LLSVP (Harpp and Weis, 2020; Jackson et al., 2018; Ritsema et al., 2011; Fig. 1). Therefore, placing constraints on the spatial distribution of lithologically distinct components in the Galápagos mantle plume, as achieved above, can be used to identify the contribution of recycled material to the deep mantle.

Seismic tomography reveals that the structure and slope of the LLSVP boundaries are not uniform (Cottaar and Lekic, 2016). For example, the boundary of the eastern Pacific LLSVP near the base of

the Galápagos mantle plume is relatively steep ($>60^\circ$), displaying a sharp transition between the LLSVP and seismically faster material to the east (Fig. 1; Frost and Rost, 2014). Conversely, the northern boundary of the Pacific LLSVP, which may represent the source region of the Hawaiian mantle plume (Weis et al., 2011), is shallower ($\sim 25\text{-}35^\circ$; Frost and Rost, 2014). These variations in the slope of the LLSVP margins have been hypothesized to result from changes in mantle dynamics and, specifically, the presence of recycled slabs in the Earth's mantle (Frost and Rost, 2014). Steeper margins, such as that observed at the eastern margin of the Pacific LLSVP, are attributed to the presence of subducted slabs, which push into the LLSVP and cause an increased thermal and compositional gradient. Additionally, a compilation of seismic tomography models indicate that there is considerable evidence to suggest that recycled slabs are present in the Earth's lowermost mantle beneath the eastern margin of the Pacific Ocean (Cottaar and Lekic, 2016; Shephard et al., 2017).

The distribution of lithologically distinct components in the Galápagos mantle plume allows us to compare the geochemical signatures of plume-related lavas to these seismic interpretations.

Geochemical evidence for pyroxenitic source components is most strongly observed in the composition of basalts from the volcanoes of northern Isabela (Ecuador and Wolf), Roca Redonda, western Santiago and Santa Cruz. These locations lie along the border between the isotopically enriched south-western domain and the isotopically depleted north-eastern domain of the Galápagos mantle plume identified by Harpp and Weis (2020). As such, our observations suggest that the Galápagos mantle plume contains a pyroxenitic, recycled component and that this component is most prevalent within the boundary zone between the enriched LLSVP material to the south-west and depleted peridotitic mantle to the north-east. It is unclear how the shallow level ($<100\text{-}200$ km depth) deflection of the Galápagos mantle plume to the north-east influences the projection of spatial variations in basalt chemistry to features in the deep mantle, but, if we assume that the spatial distribution of lower mantle material is maintained during plume ascent (Dannberg and Gassmüller, 2018; Farnetani et al., 2018), our observations suggest that subducted crustal

Accepted Article

material is present near the margin of the Pacific LLSVP and is entrained into the core of the upwelling Galápagos plume (Fig. 11). This distribution of recycled crustal material in the Pacific lower mantle can explain the localized expression of lithological heterogeneity at the surface, and is consistent with the presence of a seismically fast body near the eastern margin of the Pacific LLSVP (Frost and Rost, 2014).

Critically, there is no evidence in either the major element systematics of the Galápagos basalts, or the minor element contents of their olivine cargo, to indicate that the isotopically enriched LLSVP material melting beneath the south-western portion of the Galápagos Archipelago is pyroxenitic (Vidito et al., 2013). Consequently, there is little to no data in the Galápagos to support the popular hypothesis that the LLSVPs represent piles of subducted oceanic crust (Niu, 2018). Notably, our interpretation that the Pacific LLSVP cannot be dominated by piles of subducted oceanic crust is consistent with recent *ab initio* calculations of the density and seismic velocities of subducted crustal material, which indicate that such bodies should be visible as high velocity regions in the lower mantle (as opposed to the low seismic velocities of the LLSVPs; Wang et al., 2020). Instead, the eastern Pacific LLSVP likely contains a contribution from a primordial, or undegassed mantle component, consistent with the elevated $^3\text{He}/^4\text{He}$ signature of the Fernandina basalts. In addition, the isotopic data from the south-western Galápagos and the Loa trend of Hawaii clearly demonstrate that the LLSVP material is heterogeneous at a range of different length scales, and it is therefore unlikely that one single process is responsible for the formation of these deep mantle superstructures (Harpp and Weis, 2020; Jackson et al., 2018).

Additionally, our interpretation that recycled crustal components are external to the LLSVPs is consistent with dynamical models of mantle circulation, which demonstrate that only ~10% of subducted oceanic crust can be stored in the deep mantle superstructures (Li et al., 2014).

Therefore, the distribution of pyroxenitic components in the Galápagos mantle plume demonstrates

that recycled crustal components are present along the eastern margin of the Pacific LLSVP, and potentially contribute to the steep, sharp transition at the LLSVP margin (Frost and Rost, 2014).

7 CONCLUSIONS

The Galápagos Archipelago offers an opportunity to investigate the structure of the Earth's lower mantle and the origin of the LLSVPs through the geochemical analysis of erupted basalts. In this study we have used the major element composition of high-MgO basalts, and the minor element contents of their olivine cargo, to map out the distribution of lithologically distinct components in the Galápagos mantle plume. By comparing our results with the spatial heterogeneity in the radiogenic isotope composition of basalts from across the Archipelago we have constrained the distribution of recycled crustal components in the upwelling mantle plume and, by extension, at the core mantle boundary.

Our results indicate that the south-western and north-eastern regions of the Galápagos mantle plume, corresponding to upwelling LLSVP material and depleted mantle respectively, are dominated by peridotite, with little evidence for lithological heterogeneity. In the central and northern Galápagos, however, high FeO_t contents in primitive basalts, and Fe/Mn ratios >70 in olivine crystals, provides substantial evidence for the presence of a lithologically distinct, pyroxenitic component in the mantle source. We interpret this signature to represent the presence of recycled oceanic crust in the Galápagos mantle plume, likely dragged up from the margins of the Pacific LLSVP. We also note that there is no evidence in the geochemical composition of the Galápagos basalts to suggest that upwelling LLSVP material is lithologically distinct from the surrounding mantle. As a result, the Pacific LLSVP is unlikely to be formed through accumulation of subducted oceanic crust.

DATA AVAILABILITY STATEMENT

The data used in this study, and the python scripts used for data plotting, are available via <https://zenodo.org/badge/latestdoi/384184976>

ACKNOWLEDGEMENTS

This study was supported by a NERC (Natural Environmental Research Council) Research Training Student Grant (NE/L002507/1) and a Research Fellowship funded by the Royal Commission for the Exhibition of 1851 awarded to M.L.M.G. The Galápagos National Park authorities are acknowledged for granting SAG permission to undertake fieldwork on Isla Santiago. Staff at CDRS, together with L. Cruz and his crew, are thanked for logistical support during two field seasons on Isla Santiago. SAG also thanks those who participated in the fieldwork, including G. Estes, D. Geist, B. Manning-Geist, T. Grant, A. Miles, D. Norman and A. Thurman. The expeditions were funded by grants to SAG from the University of Cambridge, Geological Society of London and NERC (RG57434). Finally, we would like to thank Dennis Geist, William White and an anonymous reviewer for their helpful and constructive comments on this manuscript.

REFERENCES

- Allan, J.F., Simkin, T., 2000. Fernandina Volcano's evolved, well-mixed basalts: Mineralogical and petrological constraints on the nature of the Galápagos plume. *J. Geophys. Res. Solid Earth* 105, 6017–6041. <https://doi.org/10.1029/1999JB900417>
- Argus, D.F., Gordon, R.G., DeMets, C., 2011. Geologically current motion of 56 plates relative to the no-net-rotation reference frame. *Geochem. Geophys. Geosystems* 12. <https://doi.org/10.1029/2011GC003751>
- Bailey, K., 1976. Potassium-Argon Ages from the Galápagos Islands. *Science* 192, 465–467. <https://doi.org/10.1126/science.192.4238.465>
- Blichert-Toft, J., White, W.M., 2001. Hf isotope geochemistry of the Galápagos Islands. *Geochem. Geophys. Geosystems* 2. <https://doi.org/10.1029/2000GC000138>
- Bow, C.S., Geist, D.J., 1992. Geology and petrology of Floreana Island, Galápagos Archipelago, Ecuador. *J. Volcanol. Geotherm. Res.* 52, 83–105. [https://doi.org/10.1016/0377-0273\(92\)90134-Y](https://doi.org/10.1016/0377-0273(92)90134-Y)
- Brandenburg, J.P., van Keken, P.E., 2007. Deep storage of oceanic crust in a vigorously convecting mantle. *J. Geophys. Res.* 112, B06403. <https://doi.org/10.1029/2006JB004813>
- Canales, J.P., Ito, G., Detrick, R.S., Sinton, J., 2002. Crustal thickness along the western Galápagos Spreading Center and the compensation of the Galápagos hotspot swell. *Earth Planet. Sci. Lett.* 203, 311–327. [https://doi.org/10.1016/S0012-821X\(02\)00843-9](https://doi.org/10.1016/S0012-821X(02)00843-9)
- Chauvel, C., Hofmann, A.W., Vidal, P., 1992. himu-em: The French Polynesian connection. *Earth Planet. Sci. Lett.* 110, 99–119. [https://doi.org/10.1016/0012-821X\(92\)90042-T](https://doi.org/10.1016/0012-821X(92)90042-T)
- Christie, D.M., Werner, R., Hauff, F., Hoernle, K., Hanan, B.B., 2005. Morphological and geochemical variations along the eastern Galápagos Spreading Center. *Geochem. Geophys. Geosystems* 6, n/a-n/a. <https://doi.org/10.1029/2004GC000714>
- Cottaar, S., Lekic, V., 2016. Morphology of seismically slow lower-mantle structures. *Geophys. J. Int.* 207, 1122–1136. <https://doi.org/10.1093/gji/ggw324>
- Cushman, B., Sinton, J., Ito, G., Eaby Dixon, J., 2004. Glass compositions, plume-ridge interaction, and hydrous melting along the Galápagos Spreading Center, 90.5°W to 98°W. *Geochem. Geophys. Geosystems* 5. <https://doi.org/10.1029/2004GC000709>
- Dannberg, J., Gassmöller, R., 2018. Chemical trends in ocean islands explained by plume–slab interaction. *Proc. Natl. Acad. Sci.* 115, 4351–4356. <https://doi.org/10.1073/pnas.1714125115>

- Dasgupta, R., Jackson, M.G., Lee, C.-T.A., 2010. Major element chemistry of ocean island basalts — Conditions of mantle melting and heterogeneity of mantle source. *Earth Planet. Sci. Lett.* 289, 377–392. <https://doi.org/10.1016/j.epsl.2009.11.027>
- Davaille, A., Romanowicz, B., 2020. Deflating the LLSVPs: Bundles of Mantle Thermochemical Plumes Rather Than Thick Stagnant “Piles.” *Tectonics* 39. <https://doi.org/10.1029/2020TC006265>
- Deschamps, F., Cobden, L., Tackley, P.J., 2012. The primitive nature of large low shear-wave velocity provinces. *Earth Planet. Sci. Lett.* 349–350, 198–208. <https://doi.org/10.1016/j.epsl.2012.07.012>
- Detrick, R.S., Sinton, J.M., Ito, G., Canales, J.P., Behn, M., Blacic, T., Cushman, B., Dixon, J.E., Graham, D.W., Mahoney, J.J., 2002. Correlated geophysical, geochemical, and volcanological manifestations of plume-ridge interaction along the Galápagos Spreading Center. *Geochem. Geophys. Geosystems* 3, 1–14. <https://doi.org/10.1029/2002GC000350>
- Dobrovine, P.V., Steinberger, B., Torsvik, T.H., 2016. A failure to reject: Testing the correlation between large igneous provinces and deep mantle structures with EDF statistics. *Geochem. Geophys. Geosystems* 17, 1130–1163. <https://doi.org/10.1002/2015GC006044>
- Dziewonski, A.M., Woodhouse, J.H., 1987. Global Images of the Earth’s Interior. *Science* 236, 37–48. <https://doi.org/10.1126/science.236.4797.37>
- Farley, K.A., Natland, J.H., Craig, H., 1992. Binary mixing of enriched and undegassed (primitive?) mantle components (He, Sr, Nd, Pb) in Samoan lavas. *Earth Planet. Sci. Lett.* 111, 183–199. [https://doi.org/10.1016/0012-821X\(92\)90178-X](https://doi.org/10.1016/0012-821X(92)90178-X)
- Farnetani, C.G., Hofmann, A.W., Duvernay, T., Limare, A., 2018. Dynamics of rheological heterogeneities in mantle plumes. *Earth Planet. Sci. Lett.* 499, 74–82. <https://doi.org/10.1016/j.epsl.2018.07.022>
- French, S.W., Romanowicz, B., 2015. Broad plumes rooted at the base of the Earth’s mantle beneath major hotspots 19.
- Frost, D.A., Rost, S., 2014. The P-wave boundary of the Large-Low Shear Velocity Province beneath the Pacific. *Earth Planet. Sci. Lett.* 403, 380–392. <https://doi.org/10.1016/j.epsl.2014.06.046>
- Garnero, E.J., McNamara, A.K., Shim, S.-H., 2016. Continent-sized anomalous zones with low seismic velocity at the base of Earth’s mantle. *Nat. Geosci.* 9, 481–489. <https://doi.org/10.1038/ngeo2733>
- Geist, D., White, W.M., Albarede, F., Harpp, K., Reynolds, R., Blichert-Toft, J., Kurz, M.D., 2002. Volcanic evolution in the Galápagos: The dissected shield of Volcan Ecuador. *Geochem. Geophys. Geosystems* 3, 1 of 32–32 32. <https://doi.org/10.1029/2002GC000355>
- Geist, D.J., Fornari, D.J., Kurz, M.D., Harpp, K.S., Adam Soule, S., Perfit, M.R., Koleszar, A.M., 2006. Submarine Fernandina: Magmatism at the leading edge of the Galápagos hot spot. *Geochem. Geophys. Geosystems* 7. <https://doi.org/10.1029/2006GC001290>
- Geist, D.J., McBIRNEY, A.R., Duncan, R.A., 1986. Geology and petrogenesis of lavas from San Cristobal Island, Galápagos Archipelago. *Geol. Soc. Am. Bull.* 97, 555. [https://doi.org/10.1130/0016-7606\(1986\)97<555:GAPOLF>2.0.CO;2](https://doi.org/10.1130/0016-7606(1986)97<555:GAPOLF>2.0.CO;2)
- Geist, D.J., Naumann, T.R., Standish, J.J., Kurz, M.D., Harpp, K.S., White, W.M., Fornari, D.J., 2005. Wolf Volcano, Galápagos Archipelago: Melting and Magmatic Evolution at the Margins of a Mantle Plume. *J. Petrol.* 46, 2197–2224. <https://doi.org/10.1093/petrology/egi052>
- Geist, D.J., White, W.M., McBirney, A.R., 1988. Plume-asthenosphere mixing beneath the Galápagos archipelago. *Nature* 333, 657–660. <https://doi.org/10.1038/333657a0>
- Gibson, S.A., 2002. Major element heterogeneity in Archean to Recent mantle plume starting-heads. *Earth Planet. Sci. Lett.* 195, 59–74. [https://doi.org/10.1016/S0012-821X\(01\)00566-0](https://doi.org/10.1016/S0012-821X(01)00566-0)
- Gibson, S.A., Dale, C.W., Geist, D.J., Day, J.A., Brüggmann, G., Harpp, K.S., 2016. The influence of melt flux and crustal processing on Re–Os isotope systematics of ocean island basalts: Constraints from Galápagos. *Earth Planet. Sci. Lett.* 449, 345–359. <https://doi.org/10.1016/j.epsl.2016.05.021>

- Gibson, S.A., Geist, D., 2010. Geochemical and geophysical estimates of lithospheric thickness variation beneath Galápagos. *Earth Planet. Sci. Lett.* 300, 275–286. <https://doi.org/10.1016/j.epsl.2010.10.002>
- Gibson, S.A., Geist, D.G., Day, J.A., Dale, C.W., 2012. Short wavelength heterogeneity in the Galápagos plume: Evidence from compositionally diverse basalts on Isla Santiago. *Geochem. Geophys. Geosystems* 13. <https://doi.org/10.1029/2012GC004244>
- Gibson, S.A., Geist, D.J., Richards, M.A., 2015. Mantle plume capture, anchoring, and outflow during Galápagos plume-ridge interaction: Mantle plume capture & outflow. *Geochem. Geophys. Geosystems* 16, 1634–1655. <https://doi.org/10.1002/2015GC005723>
- Gibson, S.A., Richards, M.A., 2018. Delivery of deep-sourced, volatile-rich plume material to the global ridge system. *Earth Planet. Sci. Lett.* 499, 205–218. <https://doi.org/10.1016/j.epsl.2018.07.028>
- Gibson, S.A., Thompson, R.N., Dickin, A.P., 2000. Ferropicrites: geochemical evidence for Fe-rich streaks in upwelling mantle plumes. *Earth Planet. Sci. Lett.* 174, 355–374. [https://doi.org/10.1016/S0012-821X\(99\)00274-5](https://doi.org/10.1016/S0012-821X(99)00274-5)
- Gleeson, M., Gibson, S., 2021. Insights into the nature of plume-ridge interaction and outflux of H₂O from the Galápagos Spreading Centre (preprint). *Earth Sciences*. <https://doi.org/10.31223/X57P5C>
- Gleeson, M.L.M., Gibson, S.A., 2019. Crustal controls on apparent mantle pyroxenite signals in ocean-island basalts. *Geology*. <https://doi.org/10.1130/G45759.1>
- Gleeson, Matthew L M, Gibson, S.A., Stock, M.J., 2020. Upper mantle mush zones beneath low melt flux ocean island volcanoes: insights from Isla Floreana, Galápagos. *J. Petrol.* ega094. <https://doi.org/10.1093/petrology/egaa094>
- Gleeson, Matthew L.M., Gibson, S.A., Williams, H.M., 2020. Novel insights from Fe-isotopes into the lithological heterogeneity of Ocean Island Basalts and plume-influenced MORBs. *Earth Planet. Sci. Lett.* 535, 116114. <https://doi.org/10.1016/j.epsl.2020.116114>
- Global Volcanism Program, 2013. *Volcanoes of the World*, v. 4.3.4.
- Gurenko, A.A., Geldmacher, J., Hoernle, K.A., Sobolev, A.V., 2013. A composite, isotopically-depleted peridotite and enriched pyroxenite source for Madeira magmas: Insights from olivine. *Lithos* 170–171, 224–238. <https://doi.org/10.1016/j.lithos.2013.03.002>
- Gurenko, A.A., Sobolev, A.V., Hoernle, K.A., Hauff, F., Schmincke, H.-U., 2009. Enriched, HIMU-type peridotite and depleted recycled pyroxenite in the Canary plume: A mixed-up mantle. *Earth Planet. Sci. Lett.* 277, 514–524. <https://doi.org/10.1016/j.epsl.2008.11.013>
- Hanan, B.B., Graham, D.W., 1996. Lead and Helium Isotope Evidence from Oceanic Basalts for a Common Deep Source of Mantle Plumes. *Science* 272, 991–995. <https://doi.org/10.1126/science.272.5264.991>
- Harpp, K.S., Fornari, D.J., Geist, D.J., Kurz, M.D., 2003. Genovesa Submarine Ridge: A manifestation of plume-ridge interaction in the northern Galápagos Islands. *Geochem. Geophys. Geosystems* 4. <https://doi.org/10.1029/2003GC000531>
- Harpp, K.S., Geist, D.J., Koleszar, A.M., Christensen, B., Lyons, J., Sabga, M., Rollins, N., 2014a. The Geology and Geochemistry of Isla Floreana, Galápagos: A Different Type of Late-Stage Ocean Island Volcanism, in: Harpp, K.S., Mittelstaedt, E., d'Ozouville, N., Graham, D.W. (Eds.), *Geophysical Monograph Series*. John Wiley & Sons, Inc, Hoboken, New Jersey, pp. 71–117. <https://doi.org/10.1002/9781118852538.ch6>
- Harpp, K.S., Hall, P.S., Jackson, M.G., 2014b. Galápagos and Easter: A Tale of Two Hotspots, in: Harpp, K.S., Mittelstaedt, E., d'Ozouville, N., Graham, D.W. (Eds.), *Geophysical Monograph Series*. John Wiley & Sons, Inc, Hoboken, New Jersey, pp. 27–40. <https://doi.org/10.1002/9781118852538.ch3>
- Harpp, K.S., Weis, D., 2020. Insights Into the Origins and Compositions of Mantle Plumes: A Comparison of Galápagos and Hawai'i. *Geochem. Geophys. Geosystems* 21. <https://doi.org/10.1029/2019GC008887>

- Harpp, K.S., White, W.M., 2001. Tracing a mantle plume: Isotopic and trace element variations of Galápagos seamounts. *Geochem. Geophys. Geosystems* 2, n/a-n/a. <https://doi.org/10.1029/2000GC000137>
- Hauri, E.H., 1996. Major-element variability in the Hawaiian mantle plume. *Nature* 382, 415–419. <https://doi.org/10.1038/382415a0>
- Herzberg, C., 2011. Identification of Source Lithology in the Hawaiian and Canary Islands: Implications for Origins. *J. Petrol.* 52, 113–146. <https://doi.org/10.1093/petrology/egq075>
- Herzberg, C., Asimow, P.D., 2008. Petrology of some oceanic island basalts: PRIMELT2.XLS software for primary magma calculation. *Geochem. Geophys. Geosystems* 9, n/a-n/a. <https://doi.org/10.1029/2008GC002057>
- Herzberg, C., Cabral, R.A., Jackson, M.G., Vidito, C., Day, J.M.D., Hauri, E.H., 2014. Phantom Archean crust in Mangaia hotspot lavas and the meaning of heterogeneous mantle. *Earth Planet. Sci. Lett.* 396, 97–106. <https://doi.org/10.1016/j.epsl.2014.03.065>
- Herzberg, C., O'Hara, M.J., 2002. Plume-Associated Ultramafic Magmas of Phanerozoic Age. *J. Petrol.* 43, 1857–1883. <https://doi.org/10.1093/petrology/43.10.1857>
- Heyn, B.H., Conrad, C.P., Trønnnes, R.G., 2020. How Thermochemical Piles Can (Periodically) Generate Plumes at Their Edges. *J. Geophys. Res. Solid Earth* 125. <https://doi.org/10.1029/2019JB018726>
- Hirose, K., Kushiro, I., 1993. Partial melting of dry peridotites at high pressures: Determination of compositions of melts segregated from peridotite using aggregates of diamond. *Earth Planet. Sci. Lett.* 114, 477–489. [https://doi.org/10.1016/0012-821X\(93\)90077-M](https://doi.org/10.1016/0012-821X(93)90077-M)
- Hirschmann, M.M., Kogiso, Tetsu, Baker, M.B., Stolper, E.M., 2003. Alkalic magmas generated by partial melting of garnet pyroxenite 4.
- Hoernle, K., Rohde, J., Hauff, F., Garbe-Schönberg, D., Homrighausen, S., Werner, R., Morgan, J.P., 2015. How and when plume zonation appeared during the 132 Myr evolution of the Tristan Hotspot. *Nat. Commun.* 6, 7799. <https://doi.org/10.1038/ncomms8799>
- Hoernle, K., Werner, R., Morgan, J.P., Garbe-Schönberg, D., Bryce, J., Mrazek, J., 2000. Existence of complex spatial zonation in the Galápagos plume. *Geology* 28, 435. [https://doi.org/10.1130/0091-7613\(2000\)28<435:EOCSZI>2.0.CO;2](https://doi.org/10.1130/0091-7613(2000)28<435:EOCSZI>2.0.CO;2)
- Hofmann, A.W., 1997. Mantle geochemistry: the message from oceanic volcanism. *Nature* 385, 219–229. <https://doi.org/10.1038/385219a0>
- Holland, T.J.B., Green, E.C.R., Powell, R., 2018. Melting of Peridotites through to Granites: A Simple Thermodynamic Model in the System KNCFMASHTOCr. *J. Petrol.* 59, 881–900. <https://doi.org/10.1093/petrology/egy048>
- Holland, T.J.B., Powell, R., 2011. An improved and extended internally consistent thermodynamic dataset for phases of petrological interest, involving a new equation of state for solids. *J. Metamorph. Geol.* 29, 333–383. <https://doi.org/10.1111/j.1525-1314.2010.00923.x>
- Hooft, E.E.E., Toomey, D.R., Solomon, S.C., 2003. Anomalously thin transition zone beneath the Galápagos hotspot. *Earth Planet. Sci. Lett.* 216, 55–64. [https://doi.org/10.1016/S0012-821X\(03\)00517-X](https://doi.org/10.1016/S0012-821X(03)00517-X)
- Huang, S., Hall, P.S., Jackson, M.G., 2011. Geochemical zoning of volcanic chains associated with Pacific hotspots. *Nat. Geosci.* 4, 874–878. <https://doi.org/10.1038/ngeo1263>
- Humayun, M., Qin, L., Norman, M., 2004. Geochemical Evidence for Excess Iron in the Mantle Beneath Hawaii. *Science* 306, 91–94. <https://doi.org/10.1126/science.1101050>
- Ingle, S., Ito, G., Mahoney, J.J., Chazey, W., Sinton, J., Rotella, M., Christie, D.M., 2010. Mechanisms of geochemical and geophysical variations along the western Galápagos Spreading Center. *Geochem. Geophys. Geosystems* 11. <https://doi.org/10.1029/2009GC002694>
- Jackson, M.G., Becker, T.W., Konter, J.G., 2018. Geochemistry and Distribution of Recycled Domains in the Mantle Inferred From Nd and Pb Isotopes in Oceanic Hot Spots: Implications for Storage in the Large Low Shear Wave Velocity Provinces. *Geochem. Geophys. Geosystems* 19, 3496–3519. <https://doi.org/10.1029/2018GC007552>

- Jackson, M.G., Carlson, R.W., Kurz, M.D., Kempton, P.D., Francis, D., Blusztajn, J., 2010. Evidence for the survival of the oldest terrestrial mantle reservoir. *Nature* 466, 853–856. <https://doi.org/10.1038/nature09287>
- Kogiso, T., Hirschmann, M.M., Frost, D.J., 2003. High-pressure partial melting of garnet pyroxenite: possible mafic lithologies in the source of ocean island basalts. *Earth Planet. Sci. Lett.* 216, 603–617. [https://doi.org/10.1016/S0012-821X\(03\)00538-7](https://doi.org/10.1016/S0012-821X(03)00538-7)
- Kurz, M.D., Geist, D., 1999. Dynamics of the Galápagos hotspot from helium isotope geochemistry. *Geochim. Cosmochim. Acta* 63, 4139–4156. [https://doi.org/10.1016/S0016-7037\(99\)00314-2](https://doi.org/10.1016/S0016-7037(99)00314-2)
- Labrosse, S., Hernlund, J.W., Coltice, N., 2007. A crystallizing dense magma ocean at the base of the Earth's mantle. *Nature* 450, 866–869. <https://doi.org/10.1038/nature06355>
- Lambart, S., 2017. No direct contribution of recycled crust in Icelandic basalts. *Geochem. Perspect. Lett.* 7–12. <https://doi.org/10.7185/geochemlet.1728>
- Lambart, S., Baker, M.B., Stolper, E.M., 2016. The role of pyroxenite in basalt genesis: Melt-PX, a melting parameterization for mantle pyroxenites between 0.9 and 5 GPa: Melt-PX: Pyroxenite Melting Model. *J. Geophys. Res. Solid Earth* 121, 5708–5735. <https://doi.org/10.1002/2015JB012762>
- Lambart, S., Laporte, D., Provost, A., Schiano, P., 2012. Fate of Pyroxenite-derived Melts in the Peridotitic Mantle: Thermodynamic and Experimental Constraints. *J. Petrol.* 53, 451–476. <https://doi.org/10.1093/petrology/egr068>
- Lambart, S., Laporte, D., Schiano, P., 2013. Markers of the pyroxenite contribution in the major-element compositions of oceanic basalts: Review of the experimental constraints. *Lithos* 160–161, 14–36. <https://doi.org/10.1016/j.lithos.2012.11.018>
- Lau, H.C.P., Mitrovica, J.X., Davis, J.L., Tromp, J., Yang, H.-Y., Al-Attar, D., 2017. Tidal tomography constrains Earth's deep-mantle buoyancy. *Nature* 551, 321–326. <https://doi.org/10.1038/nature24452>
- Li, M., McNamara, A.K., Garnero, E.J., 2014. Chemical complexity of hotspots caused by cycling oceanic crust through mantle reservoirs. *Nat. Geosci.* 7, 366–370. <https://doi.org/10.1038/ngeo2120>
- Mahr, J., Harpp, K S, Kurz, M D, Geist, D, Bercovici, H., Pimentel, R., Cleary, Z., 2016. Rejuvenescent Volcanism on San Cristóbal Island, Galápagos: A Late "Plumer". AGU Fall Abstr.
- Mallik, A., Dasgupta, R., 2012. Reaction between MORB-eclogite derived melts and fertile peridotite and generation of ocean island basalts. *Earth Planet. Sci. Lett.* 329–330, 97–108. <https://doi.org/10.1016/j.epsl.2012.02.007>
- Matthews, S., Shorttle, O., Wong, K., 2020. simonwmatthews/pyMelt: First Release. Zenodo. <https://doi.org/10.5281/ZENODO.4011814>
- Matthews, S., Wong, K., Shorttle, O., Edmonds, M., Maclennan, J., 2021. Do Olivine Crystallization Temperatures Faithfully Record Mantle Temperature Variability? *Geochem. Geophys. Geosystems* 22. <https://doi.org/10.1029/2020GC009157>
- Matzen, A.K., Baker, M.B., Beckett, J.R., Stolper, E.M., 2013. The Temperature and Pressure Dependence of Nickel Partitioning between Olivine and Silicate Melt. *J. Petrol.* 54, 2521–2545. <https://doi.org/10.1093/petrology/egt055>
- Matzen, A.K., Baker, M.B., Beckett, J.R., Wood, B.J., Stolper, E.M., 2017b. The effect of liquid composition on the partitioning of Ni between olivine and silicate melt. *Contrib. Mineral. Petrol.* 172. <https://doi.org/10.1007/s00410-016-1319-8>
- Matzen, A.K., Wood, B.J., Baker, M.B., Stolper, E.M., 2017a. The roles of pyroxenite and peridotite in the mantle sources of oceanic basalts. *Nat. Geosci.* 10, 530–535. <https://doi.org/10.1038/ngeo2968>
- McBirney, A., Williams, H., 1969. *Geology and Petrology of the Galápagos Islands*. Geological Society of America.

- Morgan, W.J., 1971. Convection Plumes in the Lower Mantle. *Nature* 230, 42–43.
<https://doi.org/10.1038/230042a0>
- Moulik, P., Ekström, G., 2016. The relationships between large-scale variations in shear velocity, density, and compressional velocity in the Earth's mantle: LARGE-SCALE v_p , v_s , AND ρ VARIATIONS. *J. Geophys. Res. Solid Earth* 121, 2737–2771.
<https://doi.org/10.1002/2015JB012679>
- Naumann, T., 2002. Petrology and Geochemistry of Volcan Cerro Azul: Petrologic Diversity among the Western Galápagos Volcanoes. *J. Petrol.* 43, 859–883.
<https://doi.org/10.1093/petrology/43.5.859>
- Naumann, T., Geist, D., 2000. Physical volcanology and structural development of Cerro Azul Volcano, Isabela Island, Galápagos: implications for the development of Galápagos-type shield volcanoes. *Bull. Volcanol.* 61, 497–514. <https://doi.org/10.1007/s004450050001>
- Niu, Y., 2018. Origin of the LLSVPs at the base of the mantle is a consequence of plate tectonics – A petrological and geochemical perspective. *Geosci. Front.* 9, 1265–1278.
<https://doi.org/10.1016/j.gsf.2018.03.005>
- Nolet, G., Hello, Y., Lee, S. van der, Bonnieux, S., Ruiz, M.C., Pazmino, N.A., Deschamps, A., Regnier, M.M., Font, Y., Chen, Y.J., Simons, F.J., 2019. Imaging the Galápagos mantle plume with an unconventional application of floating seismometers. *Sci. Rep.* 9, 1326.
<https://doi.org/10.1038/s41598-018-36835-w>
- Peters, B.J., Carlson, R.W., Day, J.M.D., Horan, M.F., 2018. Hadean silicate differentiation preserved by anomalous $^{142}\text{Nd}/^{144}\text{Nd}$ ratios in the Réunion hotspot source. *Nature* 555, 89–93.
<https://doi.org/10.1038/nature25754>
- Powell, R., Holland, T., Worley, B., 1998. Calculating phase diagrams involving solid solutions via non-linear equations, with examples using THERMOCALC. *J. Metamorph. Geol.* 16, 577–588.
<https://doi.org/10.1111/j.1525-1314.1998.00157.x>
- Richards, F., Hoggard, M., Ghelichkhan, S., Koelemeijer, P., Lau, H., 2021. Geodynamic, geodetic, and seismic constraints favour deflated and dense-cored LLVPs (preprint). *Cosmochemistry*.
<https://doi.org/10.31223/X55601>
- Ritsema, J., Deuss, A., van Heijst, H.J., Woodhouse, J.H., 2011. S4ORTS: a degree-40 shear-velocity model for the mantle from new Rayleigh wave dispersion, teleseismic traveltimes and normal-mode splitting function measurements. *Geophys. J. Int.* 184, 1223–1236.
<https://doi.org/10.1111/j.1365-246X.2010.04884.x>
- Rosenthal, A., Yaxley, G.M., Green, D.H., Hermann, J., Kovács, I., Spandler, C., 2015. Continuous eclogite melting and variable refertilisation in upwelling heterogeneous mantle. *Sci. Rep.* 4.
<https://doi.org/10.1038/srep06099>
- Rychert, C.A., Harmon, N., Ebinger, C., 2014. Receiver function imaging of lithospheric structure and the onset of melting beneath the Galápagos Archipelago. *Earth Planet. Sci. Lett.* 388, 156–165. <https://doi.org/10.1016/j.epsl.2013.11.027>
- Saal, A., Kurz, M., Hart, S., Blusztajn, J., Blicherttoft, J., Liang, Y., Geist, D., 2007. The role of lithospheric gabbros on the composition of Galápagos lavas. *Earth Planet. Sci. Lett.* 257, 391–406. <https://doi.org/10.1016/j.epsl.2007.02.040>
- Schilling, J.-G., Kingsley, R.H., Devine, J.D., 1982. Galápagos Hot Spot-Spreading Center System: 1. Spatial petrological and geochemical variations (83°W – 101°W). *J. Geophys. Res. Solid Earth* 87, 5593–5610. <https://doi.org/10.1029/JB087iB07p05593>
- Shephard, G.E., Matthews, K.J., Hosseini, K., Domeier, M., 2017. On the consistency of seismically imaged lower mantle slabs. *Sci. Rep.* 7, 10976. <https://doi.org/10.1038/s41598-017-11039-w>
- Shorttle, O., Maclennan, J., 2011. Compositional trends of Icelandic basalts: Implications for short-length scale lithological heterogeneity in mantle plumes. *Geochem. Geophys. Geosystems* 12. <https://doi.org/10.1029/2011GC003748>
- Shorttle, O., Maclennan, J., Lambart, S., 2014. Quantifying lithological variability in the mantle. *Earth Planet. Sci. Lett.* 395, 24–40. <https://doi.org/10.1016/j.epsl.2014.03.040>

- Sinton, J., Detrick, R., Canales, J.P., Ito, G., Behn, M., 2003. Morphology and segmentation of the western Galápagos Spreading Center, 90.5°-98°W: Plume-ridge interaction at an intermediate spreading ridge. *Geochem. Geophys. Geosystems* 4. <https://doi.org/10.1029/2003GC000609>
- Sobolev, A.V., Hofmann, A.W., Kuzmin, D.V., Yaxley, G.M., Arndt, N.T., Chung, S.-L., Danyushevsky, L.V., Elliott, T., Frey, F.A., Garcia, M.O., Gurenko, A.A., Kamenetsky, V.S., Kerr, A.C., Krivolutsкая, N.A., Matvienkov, V.V., Nikogosian, I.K., Rocholl, A., Sigurdsson, I.A., Sushchevskaya, N.M., Teklay, M., 2007. The Amount of Recycled Crust in Sources of Mantle-Derived Melts 316, 7.
- Sobolev, A.V., Hofmann, A.W., Sobolev, S.V., Nikogosian, I.K., 2005. An olivine-free mantle source of Hawaiian shield basalts. *Nature* 434, 590–597. <https://doi.org/10.1038/nature03411>
- Standish, J., Geist, D., Harpp, K., Kurz, M.D., 1998. The emergence of a Galápagos shield volcano, Roca Redonda. *Contrib. Mineral. Petrol.* 133, 136–148. <https://doi.org/10.1007/s004100050443>
- Steinberger, B., Seidel, M., Torsvik, T.H., 2017. Limited true polar wander as evidence that Earth's nonhydrostatic shape is persistently triaxial. *Geophys. Res. Lett.* 44, 827–834. <https://doi.org/10.1002/2016GL071937>
- Stevenson D.S. (2019) Planetary Tectonism. In: Red Dwarfs. Springer, Cham. https://doi.org/10.1007/978-3-030-25550-3_3
- Stracke, A., Hofmann, A.W., Hart, S.R., 2005. FOZO, HIMU, and the rest of the mantle zoo. *Geochem. Geophys. Geosystems* 6. <https://doi.org/10.1029/2004GC000824>
- Stuart, F.M., Lass-Evans, S., Godfrey Fitton, J., Ellam, R.M., 2003. High $^3\text{He}/^4\text{He}$ ratios in picritic basalts from Baffin Island and the role of a mixed reservoir in mantle plumes. *Nature* 424, 57–59. <https://doi.org/10.1038/nature01711>
- Swanson, F., Baitis, H., Lexa, J., Dymond, J., 1974. Geology of Santiago, Rábida, and Pinzón Islands, Galápagos. *GSA Bull.* [https://doi.org/10.1130/0016-7606\(1974\)85%3C1803:GOSRAP%3E2.0.CO;2](https://doi.org/10.1130/0016-7606(1974)85%3C1803:GOSRAP%3E2.0.CO;2)
- Takahashi, E., Shimazaki, T., Tsuzaki, Y., Yoshida, H., 1993. Melting study of a peridotite KLB-1 to 6.5 GPa, and the origin of basaltic magmas. *Philos. Trans. R. Soc. Lond. Ser. Phys. Eng. Sci.* 342, 105–120. <https://doi.org/10.1098/rsta.1993.0008>
- Teasdale, R., Geist, D., Kurz, M., Harpp, K., 2005. 1998 Eruption at Volcán Cerro Azul, Galápagos Islands: I. Syn-Eruptive Petrogenesis. *Bull. Volcanol.* 67, 170–185. <https://doi.org/10.1007/s00445-004-0371-9>
- Trela, J., Vidito, C., Gazel, E., Herzberg, C., Class, C., Whalen, W., Jicha, B., Bizimis, M., Alvarado, G.E., 2015. Recycled crust in the Galápagos Plume source at 70 Ma: Implications for plume evolution. *Earth Planet. Sci. Lett.* 425, 268–277. <https://doi.org/10.1016/j.epsl.2015.05.036>
- Vidito, C., Herzberg, C., Gazel, E., Geist, D., Harpp, K., 2013. Lithological structure of the Galápagos Plume. *Geochem. Geophys. Geosystems* 14, 4214–4240. <https://doi.org/10.1002/ggge.20270>
- Villagómez, D.R., Toomey, D.R., Geist, D.J., Hooft, E.E.E., Solomon, S.C., 2014. Mantle flow and multistage melting beneath the Galápagos hotspot revealed by seismic imaging. *Nat. Geosci.* 7, 151–156. <https://doi.org/10.1038/ngeo2062>
- Wang, W., Xu, Y., Sun, D., Ni, S., Wentzcovitch, R., Wu, Z., 2020. Velocity and density characteristics of subducted oceanic crust and the origin of lower-mantle heterogeneities. *Nat. Commun.* 11, 64. <https://doi.org/10.1038/s41467-019-13720-2>
- Weis, D., Garcia, M.O., Rhodes, J.M., Jellinek, M., Scoates, J.S., 2011. Role of the deep mantle in generating the compositional asymmetry of the Hawaiian mantle plume. *Nat. Geosci.* 4, 831–838. <https://doi.org/10.1038/ngeo1328>
- White, W.M., Hofmann, A.W., 1982. Sr and Nd isotope geochemistry of oceanic basalts and mantle evolution. *Nature* 296, 821–825. <https://doi.org/10.1038/296821a0>

- White, W.M., McBirney, A.R., Duncan, R.A., 1993. Petrology and geochemistry of the Galápagos Islands: Portrait of a pathological mantle plume. *J. Geophys. Res. Solid Earth* 98, 19533–19563. <https://doi.org/10.1029/93JB02018>
- Wieser, P.E., Edmonds, M., Maclennan, J., Jenner, F.E., Kunz, B.E., 2019. Crystal scavenging from mush piles recorded by melt inclusions. *Nat Commun* 10, 5797. <https://doi.org/10.1038/s41467-019-13518-2>
- Willbold, M., Stracke, A., 2006. Trace element composition of mantle end-members: Implications for recycling of oceanic and upper and lower continental crust. *Geochem. Geophys. Geosystems* 7, n/a-n/a. <https://doi.org/10.1029/2005GC001005>
- Wilson, J.T., 1973. Mantle plumes and plate motions. *Tectonophysics* 19, 149–164. [https://doi.org/10.1016/0040-1951\(73\)90037-1](https://doi.org/10.1016/0040-1951(73)90037-1)
- Yaxley, G.M., Green, D.H., 1998. Reactions between eclogite and peridotite: mantle refertilisation by subduction of oceanic crust. *Schweiz Miner. Petrogr Mitt* 78, 243–255.
- Zhou, H., Hoernle, K., Geldmacher, J., Hauff, F., Homrighausen, S., Garbe-Schönberg, D., Jung, S., 2020. Geochemistry of Etendeka magmatism: Spatial heterogeneity in the Tristan-Gough plume head. *Earth Planet. Sci. Lett.* 535, 116123. <https://doi.org/10.1016/j.epsl.2020.116123>

FIGURE CAPTIONS

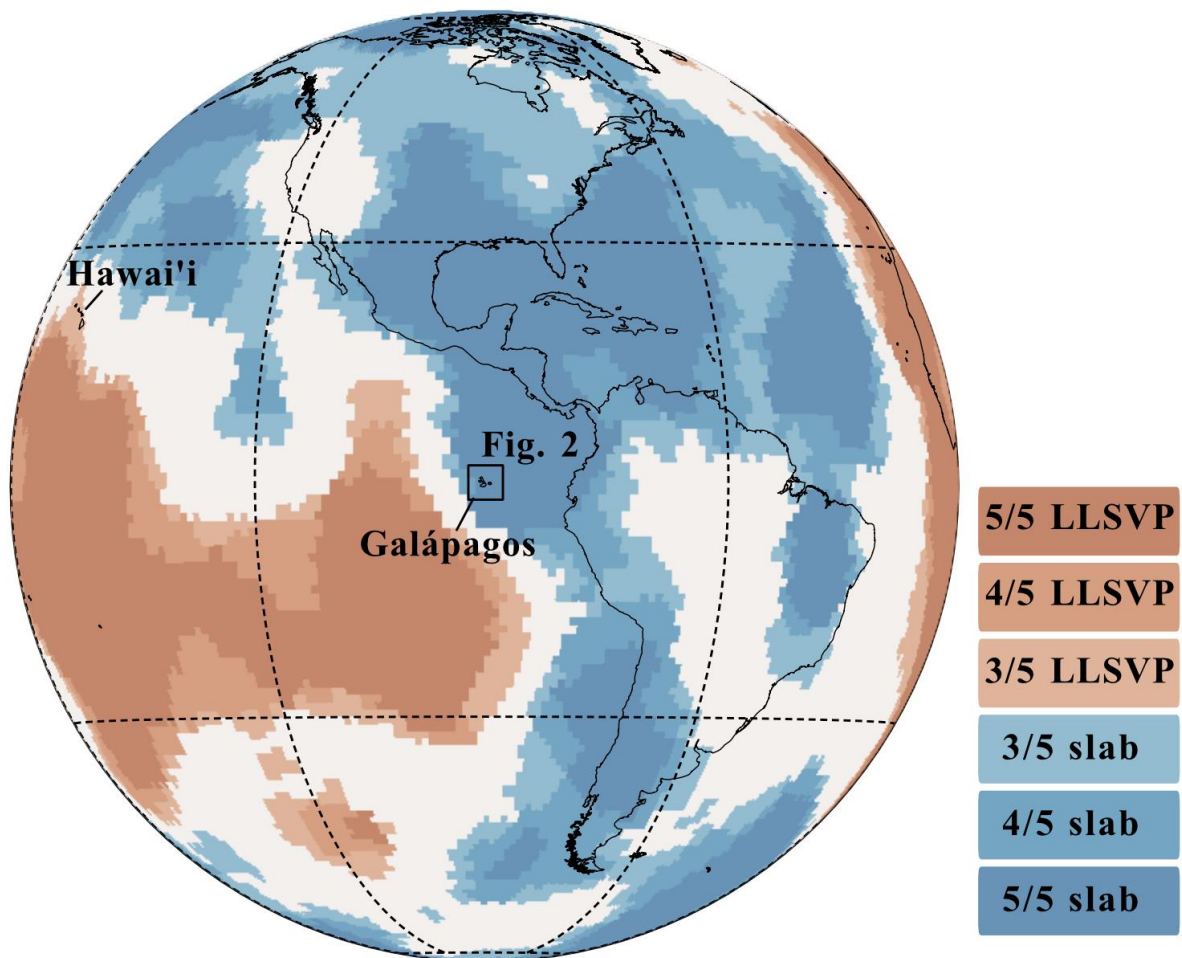


Figure 1 – Coloured regions on the map show where different tomographic models agree on the lowermost mantle being slow (red colours) and fast (blue colours) (Cottaar and Lekic, 2016, see reference therein for the five tomographic models included). Slow regions are defined as LLSVPs while fast regions are generally interpreted as subducted slab material. The geographic location of the Galápagos Archipelago is located near the NW-SE striking boundary between these two regions at the core-mantle boundary.

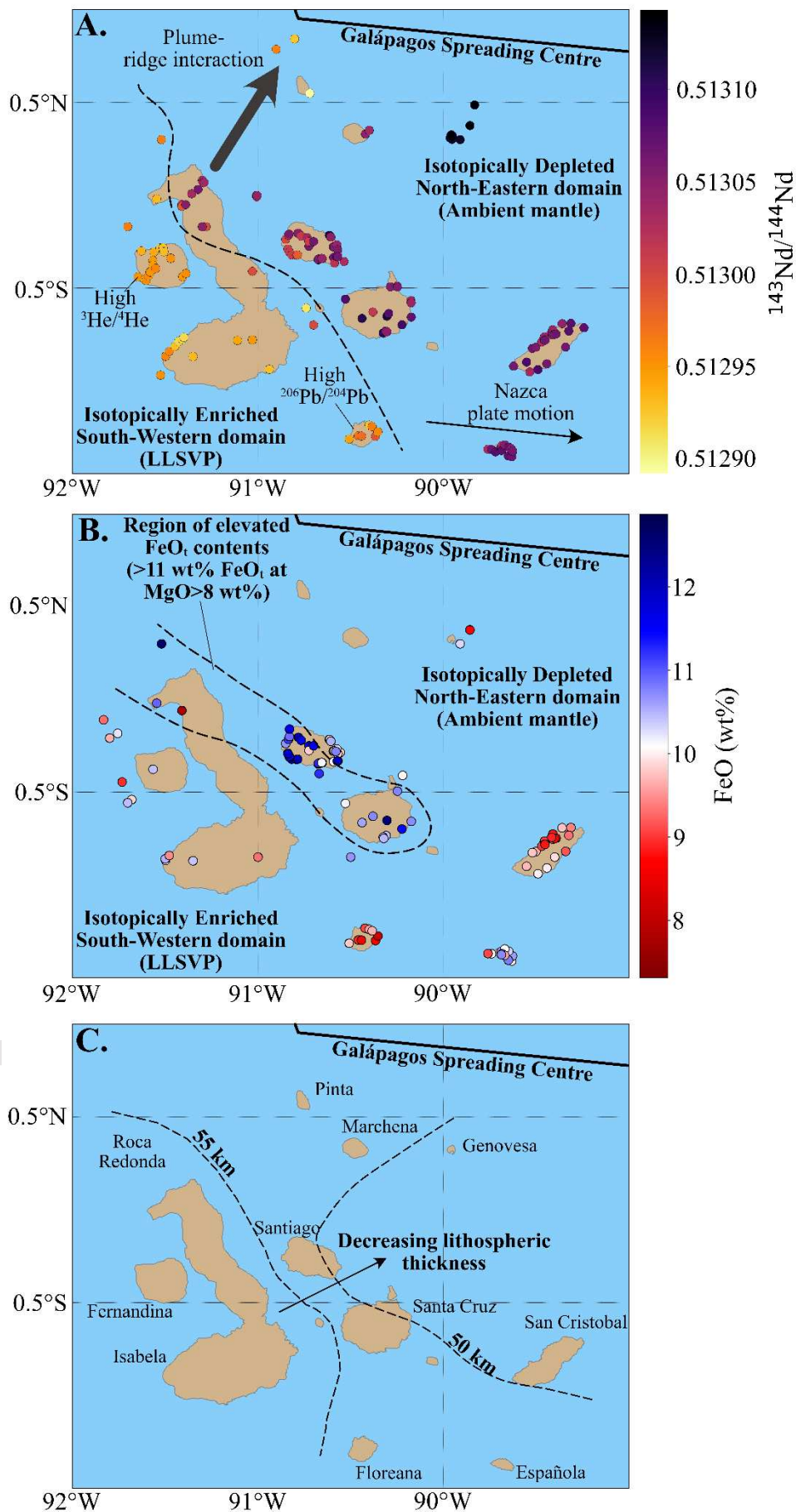


Figure 2 – Variation in the composition of basalts erupted across the Galápagos Archipelago. **A.**

Spatial variations in the $^{143}\text{Nd}/^{144}\text{Nd}$ composition of the Galápagos basalts. Less radiogenic, and thus more enriched, Nd isotope signatures are observed in the south-western Galápagos. The enriched isotopic signature of Pinta is likely related to the transfer of compositionally enriched melts to the nearby Galápagos Spreading Centre (Gleeson and Gibson, 2021). **B.** Variations in the FeO_t content of high-MgO basalts erupted in the Galápagos (basalts with MgO contents above 8 wt% are shown). Notably, areas with the highest FeO_t contents are found in the north and central Galápagos, on the islands of Santiago, Santa Cruz, Roca Redonda, and on the northern margins of Isabela. **C.** Contours of lithospheric thickness (taken from Gibson and Geist 2010) that reveal the thickness of the lithosphere decreases eastwards in the Galápagos Archipelago. Data from Allan and Simkin, 2000; Bow and Geist, 1992; Geist et al., 2002, 2006, 2005; Gibson et al., 2012; Gibson and Geist, 2010; Harpp et al., 2003; Harpp and Weis, 2020; Kurz and Geist, 1999; McBirney and Williams, 1969; Naumann et al., 2002; Saal et al., 2007; Standish et al., 1998; Swanson et al., 1974; Teasdale et al., 2005; and White et al., 1993.

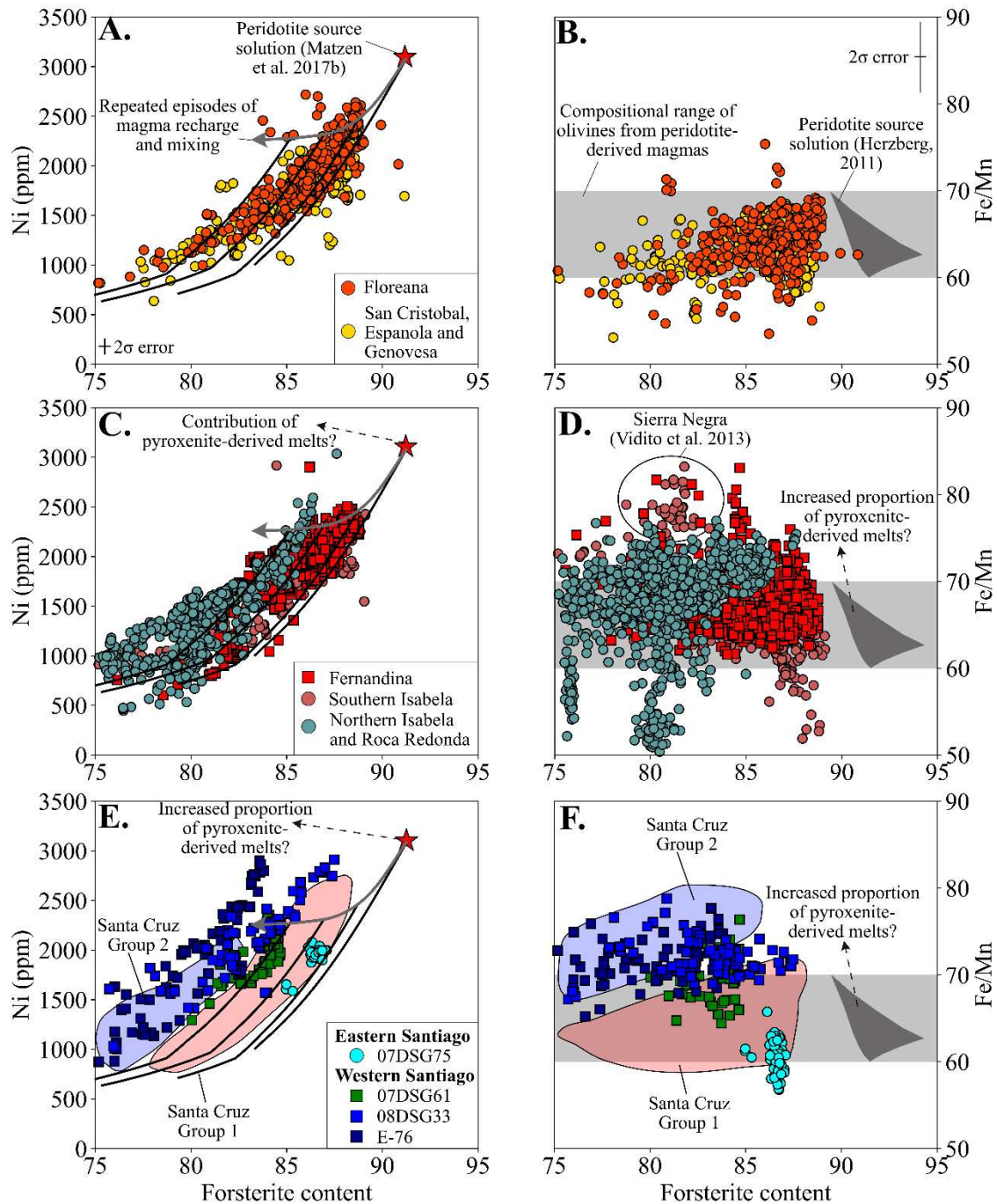


Figure 3 – Composition of olivines from the eastern and southern Galápagos (**A.**, **B.**), western Galápagos (**C.**, **D.**), and central Galápagos (**E.**, **F.**). **A.** Ni contents of olivines from islands in the eastern Galápagos (Genovesa, Espanola, and San Cristobal) and Floreana in the southern Galápagos are consistent with the compositions predicted to form from melts of a peridotite source. Data from the western Galápagos (panels **C.** and **D.**) is typically consistent with the presence of a peridotitic

source. The Ni and Fe/Mn contents of olivines from northern Isabela and Roca Redonda, however, are difficult to explain without invoking the presence of a lithologically distinct source component. Olivine data from the central Galápagos (E. and F.) is more complex, the composition of olivines in tholeiitic basalts from Santiago and Group 1 olivines from Santa Cruz are consistent with a peridotitic source. Group 2 olivines from Santa Cruz and olivines in mildly alkaline basalts from Santiago, however, require the presence of a lithologically distinct component in their mantle source. Fractional crystallisation paths in A., C., and E. are taken from Gleeson and Gibson (2019). The range of olivine Fe/Mn contents that are consistent with derivation from a peridotite source is taken from (Herzberg, 2011). Peridotite source component taken from Matzen et al. (2017b) and Herzberg (2011). Data from this study, Vidito et al. (2013), and Gleeson and Gibson (2019).

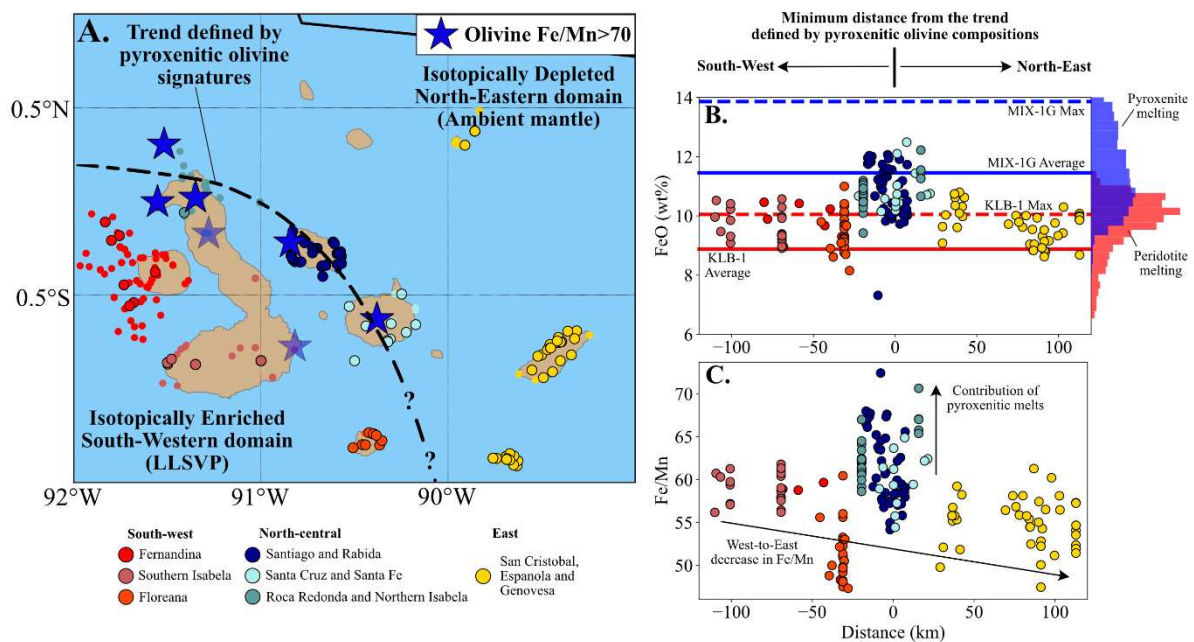


Figure 4 – Major element systematics of the Galápagos basalts. **A.** Location of basalts considered in this study, those with MgO contents above 8 wt% are displayed with a black outline. Samples with olivine Fe/Mn > 70 are highlighted by the blue stars. Samples from Sierra Negra and Darwin are partially transparent as the olivines measured from these volcanoes are very evolved. The black line represents the approximate trend through this region with ‘pyroxenitic’ olivine compositions. Basalts are broadly sub-divided into 3 categories: south-western basalts (reds); north-central basalts (blues);

and eastern basalts (yellow). **B.** The FeO_t contents of high-MgO basalts are compared to their minimum distance to the black line plotted in **A.** (i.e., the location of basalts with 'pyroxenitic' olivine compositions). We find that the FeO_t content of basalts from the south-western Galápagos and the north-eastern Galápagos are relatively constant, typically between 9 and 10.5 wt%. Notably, these FeO_t contents are consistent with those measured in experimental melts of the KLB-1 peridotite (Hirose and Kushiro, 1993; Takahashi et al., 1993) and THERMOCALC v3.4.7 calculations of melting the KLB-1 peridotite (red histogram). Basalts from the north-central Galápagos, which plot within ~25 km of the black line shown in **A.**, have higher FeO_t contents, up to 12.8 wt%. Such high FeO_t contents require the presence of lithological heterogeneity in the mantle source. The average and max FeO_t content of melting experiments on the pyroxenitic lithology MIX-1g is shown for reference (Hirschmann et al., 2003; Kogiso et al., 2003), and the FeO_t contents predicted for melting of the MIX-1g pyroxenite in THERMOCALC v3.4.7 is shown by the blue histogram. **C.** The Fe/Mn ratio of high-MgO basalts from across the Galápagos shows a general decrease from west to east. Notable exceptions to this trend are the basalts from the north-central Galápagos. Data from Allan and Simkin, 2000; Bow and Geist, 1992; Geist et al., 2002, 2006, 2005; Gibson et al., 2012; Gibson and Geist, 2010; Harpp et al., 2003; Harpp and Weis, 2020; Kurz and Geist, 1999; McBirney and Williams, 1969; Naumann et al., 2002; Saal et al., 2007; Standish et al., 1998; Swanson et al., 1974; Teasdale et al., 2005; and White et al., 1993.

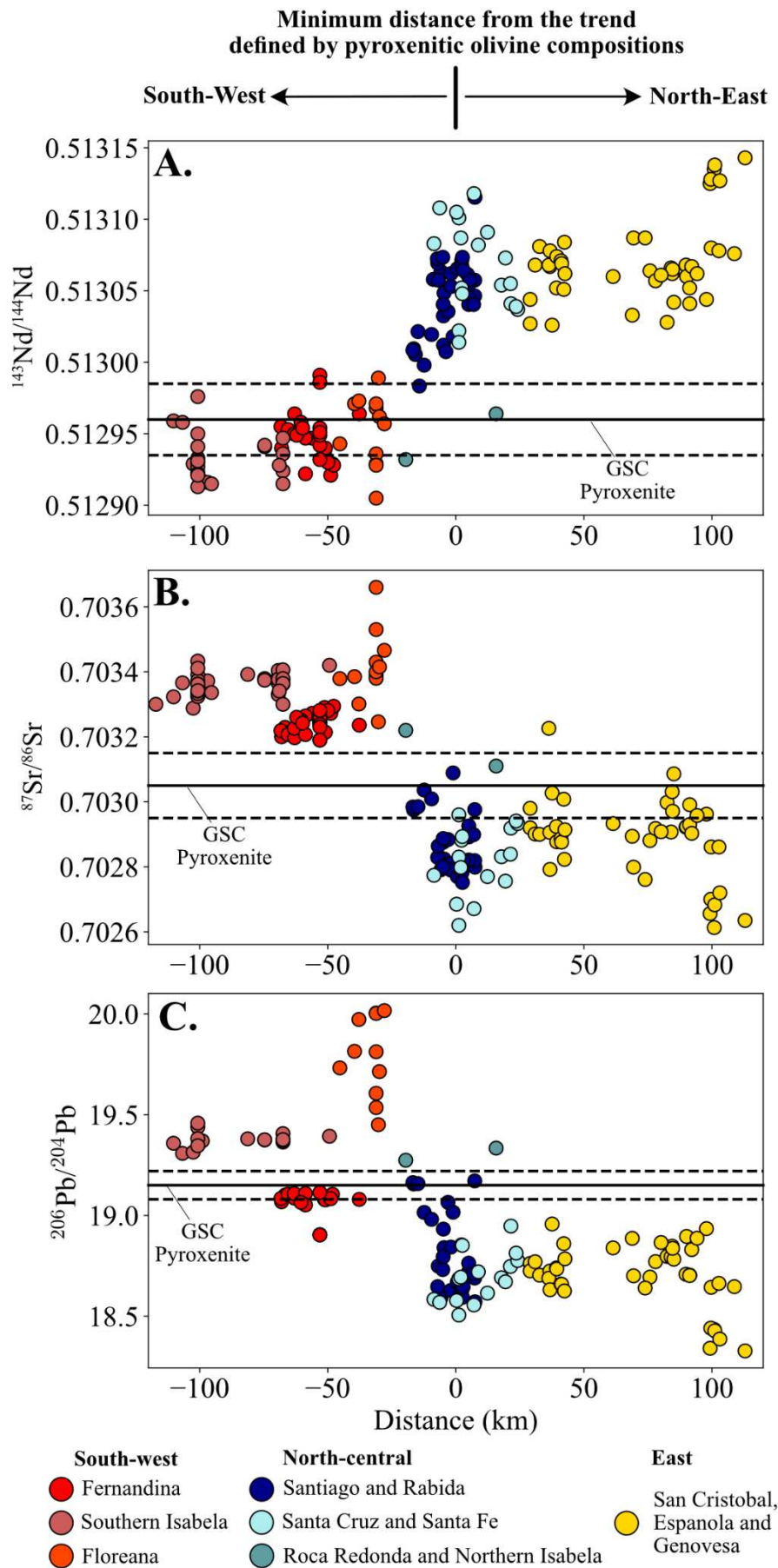


Figure 5 – Radiogenic isotope composition of basalts from the Galápagos Archipelago. In all panels, the proposed isotopic composition of the pyroxenite component in the source region of the Galápagos Spreading Centre basalts is shown by the black horizontal lines. These values are taken from the work of Gleeson et al. (2020) and Gleeson and Gibson (2021) and the uncertainties in these isotopic compositions were constrained using the python code presented in Gleeson and Gibson (2021). Basalts from Roca Redonda, northern Isabela, and the most enriched basalts from Santiago, have very similar isotopic systematics to this proposed end-member. Data from Allan and Simkin, 2000; Bow and Geist, 1992; Geist et al., 2002, 2006, 2005; Gibson et al., 2012; Gibson and Geist, 2010; Harpp et al., 2003; Harpp and Weis, 2020; Kurz and Geist, 1999; McBirney and Williams, 1969; Naumann et al., 2002; Saal et al., 2007; Standish et al., 1998; Swanson et al., 1974; Teasdale et al., 2005; and White et al., 1993.

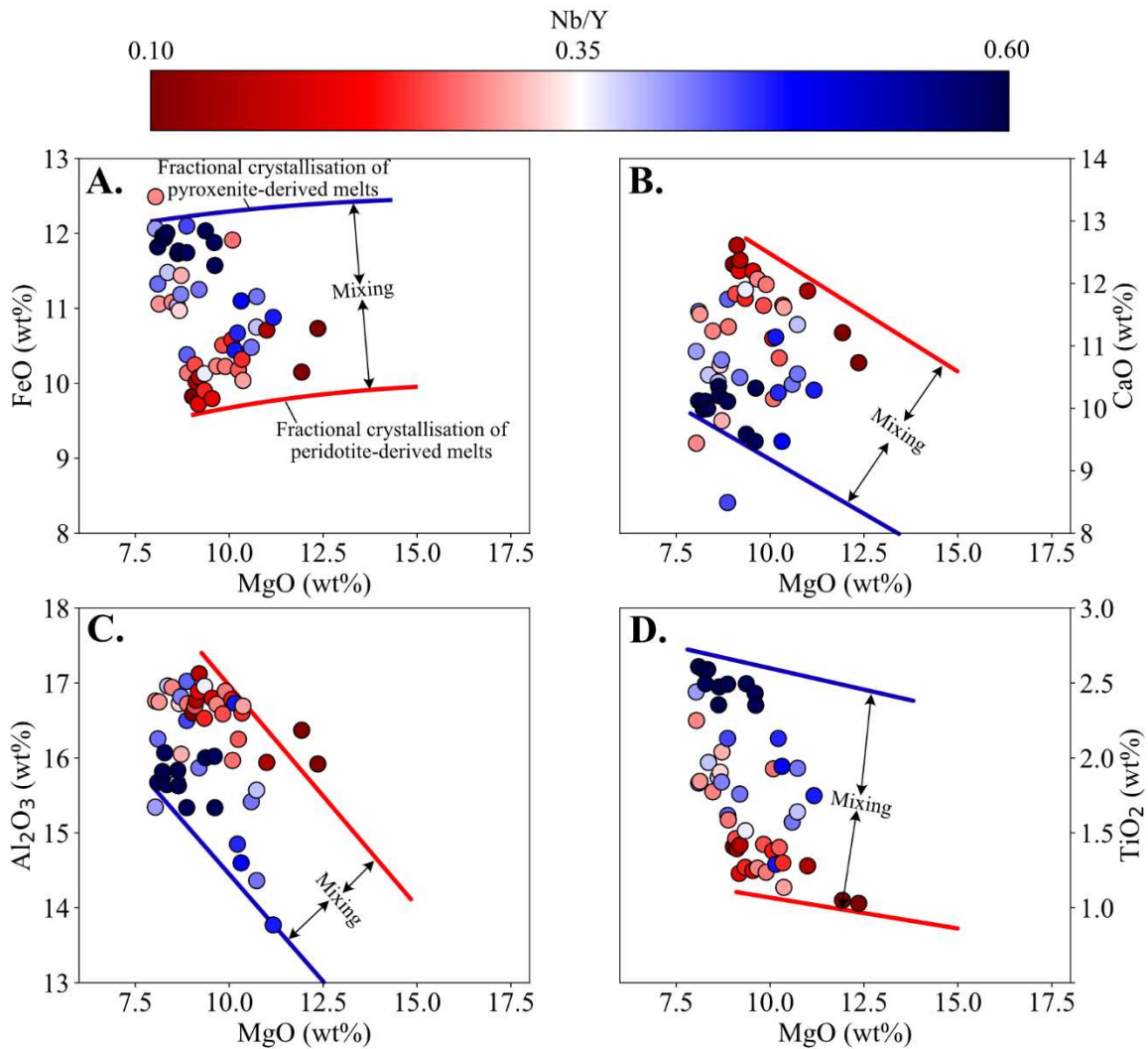


Figure 6 – Major element systematics of basalts from Santiago, Santa Cruz, Rabida and Santa Fe with MgO contents >8 wt%. The major element systematics of the high-MgO basalts are related to their isotopic and trace element signatures (represented here by their Nb/Y ratio). Pyroxenite melts contain high FeO_t and TiO₂, but lower CaO and Al₂O₃ contents than the peridotitic melts, consistent with experimental data (Lambart et al., 2013). Blue and red lines display the olivine fractionation curves, calculated by removing olivine whose composition is calculated using the olivine K_d of Herzberg and O’Hara (2002), for hypothetical pyroxenite-derived and peridotite-derived melts, respectively. Data from Gibson et al., 2012; Gibson and Geist, 2010; Harpp and Weis, 2020; McBirney and Williams, 1969; Saal et al., 2007; and White et al., 1993.

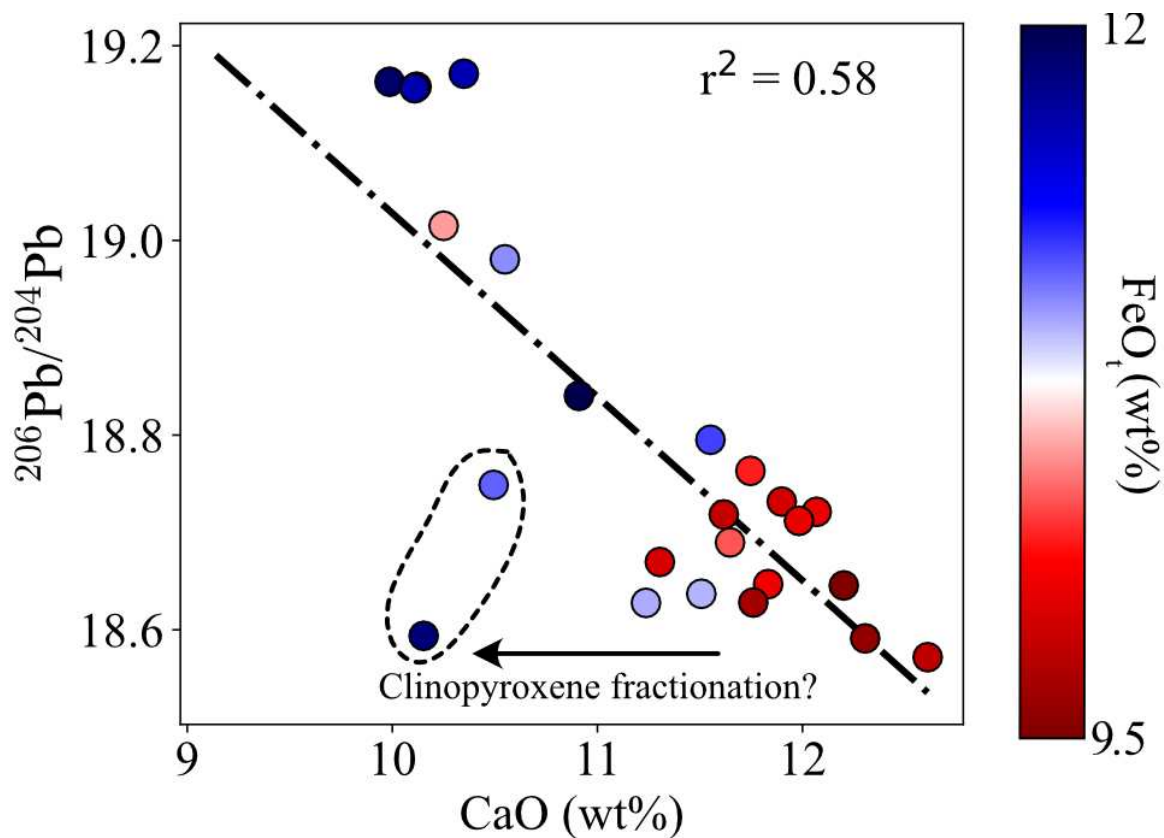


Figure 7 – Correlation between the major element systematics of the high-MgO Santiago basalts (MgO >8 wt%) and radiogenic isotopes. Strong correlations that are significant at the 99% confidence level are observed between CaO or FeO_t and the radiogenic isotope ratios considered in this study ($^{87}\text{Sr}/^{86}\text{Sr}$, $^{143}\text{Nd}/^{144}\text{Nd}$, $^{206}\text{Pb}/^{204}\text{Pb}$) and confirm the relationship between isotopic enrichment and pyroxenitic contribution in the central Galápagos. Two samples with low CaO contents and unradiogenic $^{206}\text{Pb}/^{204}\text{Pb}$ signatures might result from unfiltered clinopyroxene fractionation, but we expect the influence of plagioclase and clinopyroxene fractionation to be minor in most Galápagos basalts considered here (see Supplementary Information). Data from Gibson et al. (2012).

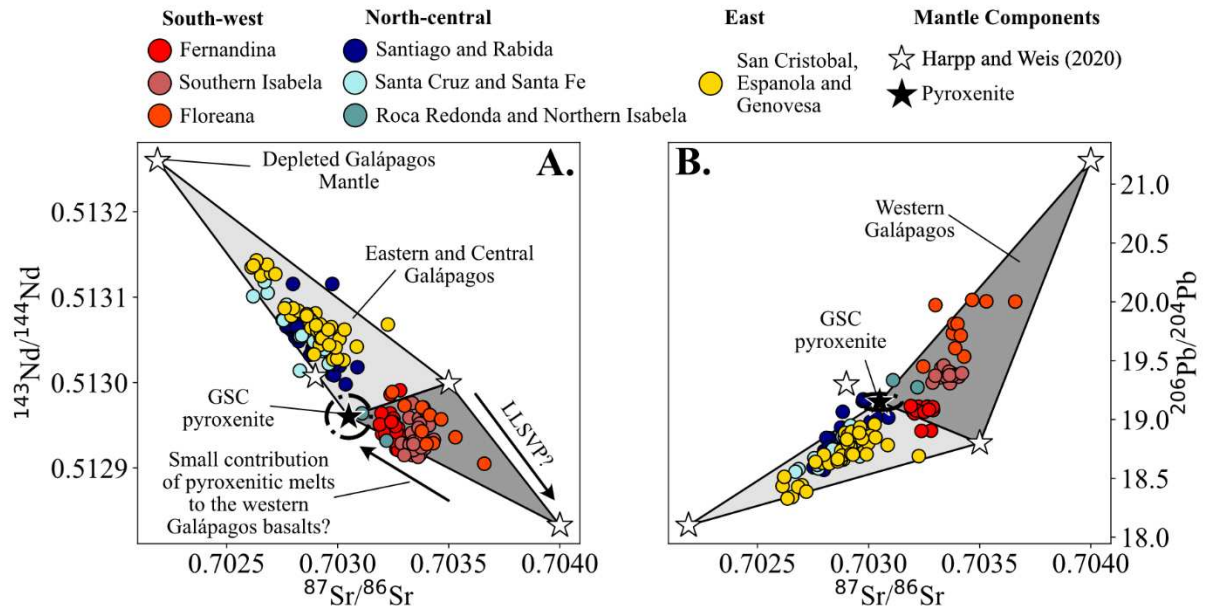


Figure 8 – Isotopic composition of the Galápagos basalts compared to the proposed mantle end-members from Harpp and Weis (2020) and the proposed isotopic composition of the Galápagos pyroxenite component (determined using the models presented by Gleeson and Gibson (2021)). There is a clear divide between the isotopic composition of basalts from the south-western Galápagos and those from the central and eastern Galápagos. We suggest that the isotopic composition of basalts from the eastern and central Galápagos are controlled by mixing of melts from the DGM and the proposed pyroxenitic end-member (potentially with a minor contribution from LLSVP material). On the other hand, basalts from the south-western Galápagos are primarily sourced from LLSVP material, but small contributions of pyroxenitic material may influence their isotopic systematics.

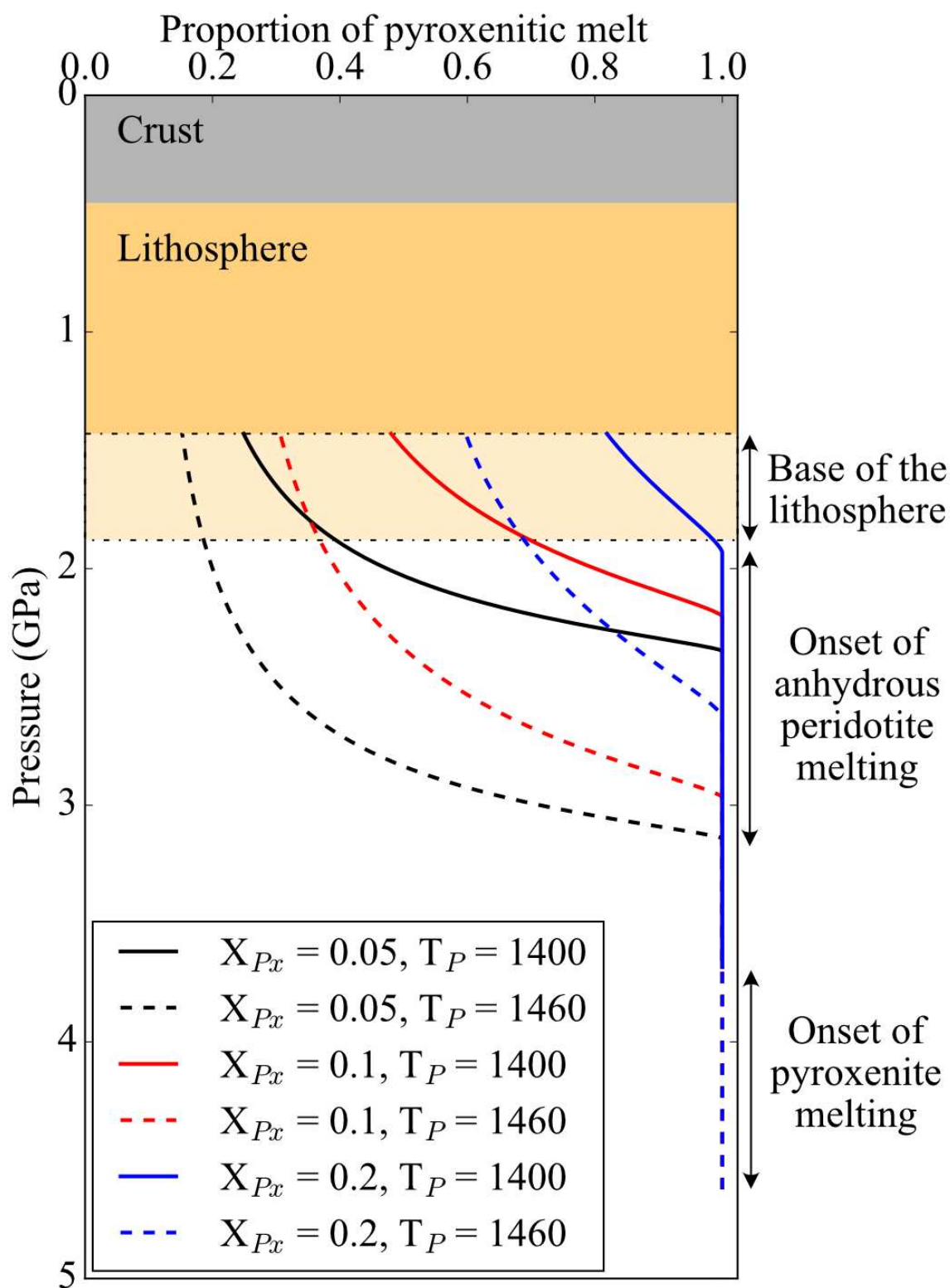


Figure 9 – Proportion of pyroxenitic melt predicted from melting of a two-component mantle.

Calculations were performed in the pymelt module (Matthews et al., 2020) over a range of initial parameters, including the proportion of pyroxenite (formed as the reaction product of melts of

subducted oceanic crust and peridotite) in the source (X_{Px}), the mantle potential temperature (T_p), and the pressure at the base of the lithosphere.

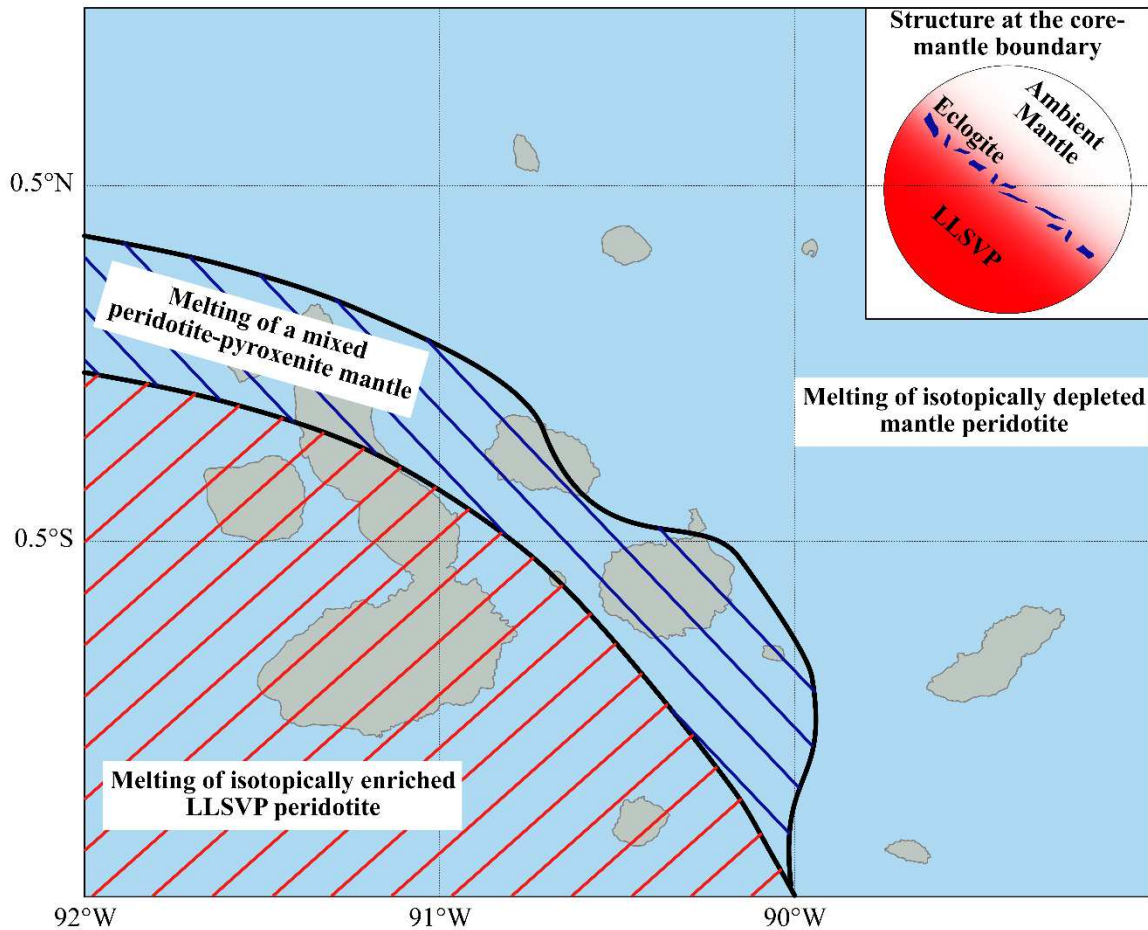


Figure 10 – Distribution of peridotite and pyroxenite in the mantle source region of the Galápagos basalts. The isotopically enriched mantle beneath the south-western Galápagos displays no evidence for lithological heterogeneity and is thus interpreted to be peridotitic. As a result, there is no evidence in the Galápagos to suggest that the Pacific LLSVP represents a pile of subducted oceanic crust. In the north-central Galápagos the chemistry of the erupted basaltic lavas is controlled by mixing of melts from a pyroxenitic mantle source, formed through the reaction of melts from subducted oceanic crust (eclogite) with surrounding mantle peridotite, and upwelling mantle

peridotite. In the eastern Galápagos, the depleted nature of the basalts indicates that the mantle source is dominated by isotopically depleted peridotitic mantle.

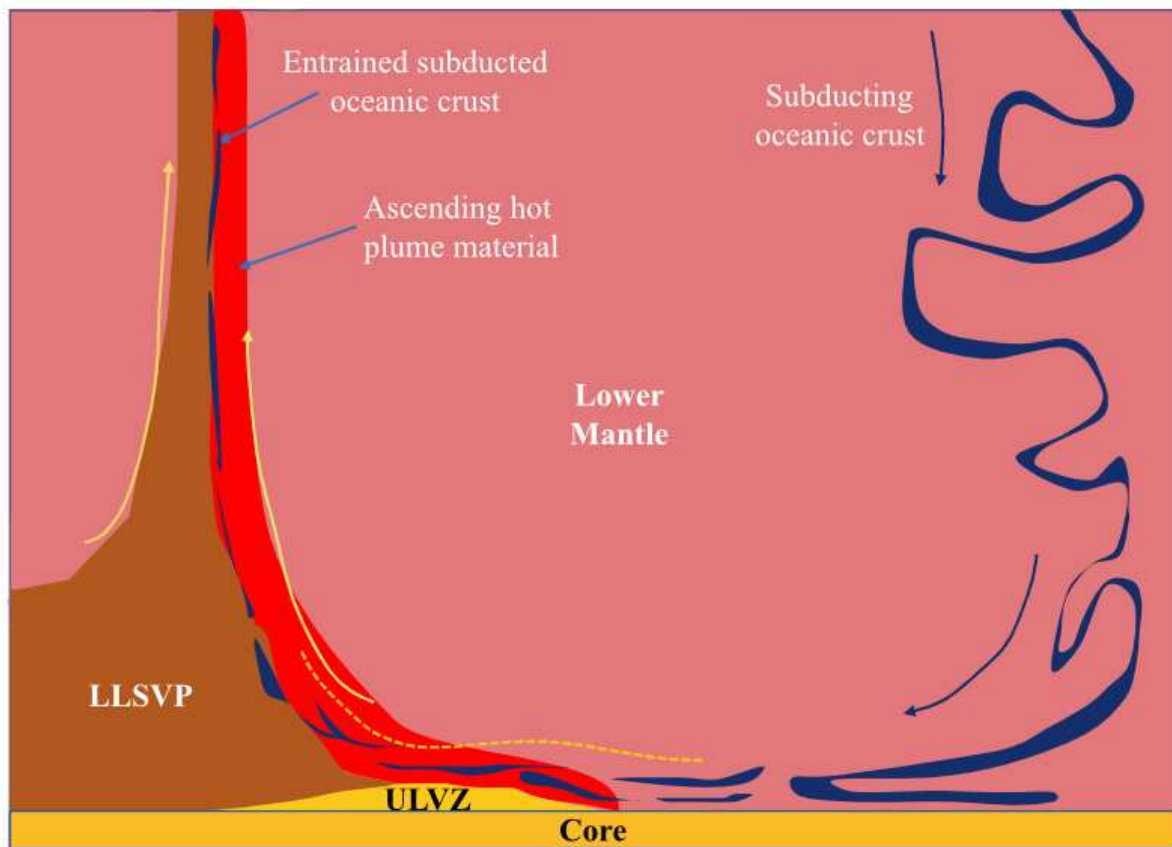


Figure 11 – Schematic of the possible structure of the Pacific LLSVP margin at the base of the Galápagos mantle plume. Subducted oceanic lithosphere is present near the margin of the LLSVP leading to the steep LLSVP margin and the spatial distribution of lithological heterogeneity in the Galápagos mantle plume. The Galápagos plume has a complex asymmetric structure, with peridotitic mantle rising on the north-eastern side of the plume and enriched LLSVP material rising on the south-western side. The LLSVP is likely formed from primordial material. Figure adapted from Stevenson (2019).